SYNTHESIS OF PLATINUM NANOSTRUCTURES USING ZEOLITES

by

Leonel Eduardo Quiñones Fontalvo

A dissertation submitted in partial fulfillment of the requirements for the degree of

DOCTOR OF PHILOSOPHY
in
CHEMICAL ENGINEERING

UNIVERSITY OF PUERTO RICO
MAYAGÜEZ CAMPUS
2011

Approved by:

_____	_____
María Martínez Iñesta, PhD President, Graduate Committee	Date
_____	_____
Arturo Hernández Maldonado, PhD Member, Graduate Committee	Date
_____	_____
Carlos Rinaldi Ramos, PhD Member, Graduate Committee	Date
_____	_____
O. Marcelo Suárez, PhD Member, Graduate Committee	Date
_____	_____
Ricky Valentín, PhD Graduate Studies Representative	Date
_____	_____
David Suleiman, PhD Chairperson of the Department	Date

THIS DISSERTATION IS DEDICATED TO MY FAMILY

ABSTRACT

Due to their outstanding and tunable electronic properties, platinum nanowires have the potential to be used in the development of advanced devices. The quantum confinement effect of the electrons and the increased surface area to volume ratio found in nanowires give them unique physical and chemical characteristics. However, until recently, the advance in the utilization of nanowires had been relatively slow due to the difficulties associated with the synthesis of such nanostructures with well-controlled size.

This dissertation shows how zeolites could be used for the synthesis of platinum nanowires as well as other nanostructures such as nanoclusters, multipods and nanoflower-like structures by using different precursors and reduction methods. In particular this dissertation shows the development of a new synthesis protocol that allows the formation of platinum nanowires in zeolites via solid state reduction.

In addition to the synthesis and characterization of the nanostructures this dissertation includes a multivariate statistical analysis of the results using the method Project to Latent Structures Discriminant Analysis.

RESUMEN

Los nanocables de platino, debido a sus atractivas propiedades electrónicas, tienen el potencial para ser utilizados en el desarrollo de equipos avanzados. Los efectos de confinamiento cuántico del electrón y el incremento de la relación área superficie a volumen hacen que los nanocables tengan propiedades físico químicas únicas. Sin embargo, hasta hace poco, los avances en la utilización de los nanocables ha sido relativamente lenta, debido a las dificultades asociadas con la síntesis de estas nanoestructuras, tales como: el control del tamaño, la cristalinidad y la composición química.

En esta disertación se muestra cómo las zeolitas pueden utilizarse para sintetizar nanocables de platino así como nanoparticulas, multipodos y estructuras parecidas a las nanoflores usando diferentes precursores y métodos de reducción. En particular esta disertación enseña el desarrollo de un protocolo de síntesis que permite la síntesis de nanocables dentro de zeolitas via reducción en estado sólido.

En adición a la síntesis y caracterización de nanoestructuras, esta disertación incluye un análisis multivariable estadístico de de los resultados usando el método Proyección a Estructuras Latentes: Análisis Discriminante.

Table of Contents

List of Tables

Tables **Page**

List of Figures

Figures **Page**

PREFACE

The motivation of this project was to develop a synthesis protocol to obtain metal nanowires using zeolites.

In Chapter 1 there is an introduction and motivation for this dissertation and also includes the fundamental concepts needed to understand the dissertation work.

Chapter 2 is centered on the study of the growth of platinum nanostructures in zeolites using non-traditional reduction techniques in the gas, liquid, and solid state that have been successful in the synthesis of Pt nanowires.

Chapter 3 and Chapter 4 present in-depth studies of the solid state reduction method. In these chapters, the effect of the concentration of sodium borohydrate, the effect of the zeolite, metal precursor charge, and the concentration of the metal in the formation of platinum nanostructures in the zeolite were evaluated. These studies allow the identification of the factors that are critical for the formation of platinum nanowires in zeolites with this method. Based on the experimental results a formation mechanism of platinum nanowires was proposed.

Chapter 5 shows a Projection of Latent Structures multivariable statistical analysis of the most relevant experimental results obtained in this research. This analysis was done to have a quantitative understanding of the relative relevance the various synthesis parameters had on the final morphology of the nanoparticles.

In the last chapter, Chapter 6, there is a summary of the most relevant conclusions obtained in this work and recommendations for future work.

During the course of this research there were key people that facilitated the use of instruments that were necessary for the fulfillment of this dissertation. These people were: Dr. Maxime Guinel from University of Puerto Rico(UPR)-Río Piedras, John Grazul from Cornell University and Dr. Arturo Hernández and Dr. Carlos Rinaldi from the UPR-Mayagüez. Funding of this research was provided by the NSF funded Institute of Functional Nanomaterials, the NSF funded Mayagüez-Wisconsin PREM and the University of Puerto Rico- Mayagüez.

Chapter 1 INTRODUCTION

Environmental pollution, diminishing fossil fuel reserves and high oil costs have driven the search of new methods for more efficient energy conversion and less environmental impact. Among the alternatives are the use of fuel cells and devices that can produce hydrogen by catalytically splitting water [1-3]. In these technologies the use of platinum nanostructures is essential due to its electrocatalytic activity and stability [1, 3, 4]. Moreover, platinum nanostructures have been studied for applications such as for biosensors [5], drug delivery [6, 7], cancer treatment [8, 9], oil refining [10] and data storage [11].

Platinum, however, is a precious metal, and its high cost demands its efficient usage for commercial applications. As the performance of platinum nanostructures is essentially dependent on the shape and size of platinum nanoparticles [1] studies focused on the control of its size and morphology at the nanoscale can help optimize platinum usage [2, 3].

Among nanostructures, nanowires, by virtue of their size and structural one-dimensionality, could allow the electrons to exhibit quantum confinement effects in the axial direction [12]. These effects could be used to develop new device concepts and enable unique applications [3, 12, 13]. Unfortunately, the progress in the utilization of nanowires has been relatively slow, due to difficulties in developing synthesis procedures that promote well-controlled size, phase purity, crystallinity, and chemical composition [12].

Platinum nanowires are currently being researched for integration into nanoelectronics and biosensors and they have shown better performance than commercially available devices [14-16].

Many research efforts have focused on the use of templates for successful synthesis of platinum nanowires and other metal nanostructures using a bottom-up approach [17-21]. The method consists first of incorporating a precursor of the desired metal into a porous material. Then, by a chemical reaction, the metal precursor is reduced to its metal form taking the one dimensional shape of the porous template.

One of the most widely used porous template to form metal nanowires is anodic aluminum oxide, typically has pore sizes larger than 50 nm [15]. Several metal nanowires have also been successfully synthesized inside the channels of mesoporous silica materials using template methods. These materials can be synthesized with pore sizes ranging 2 to 50 nm. They differ from zeolites in the pore size range and in that their pore walls are amorphous. Among the mesoporous materials studied for the

synthesis of metals nanowires are MCM-48 [22], SBA-15 [23], FSM-16 [18] and HMM [20, 21].

Among template materials, zeolites offer an appealing option, because they can be synthesized with 1, 2, and 3 dimensional pores with diameters ranging between 0.4 nm and 1.2 nm. The synthesis of metal nanowires using zeolitic materials as templates would potentially yield nanostructures with novel morphologies that could promote the development of new technologies and increase the efficiency in current applications [1, 24].

The use of zeolites for the synthesis of nanostructures has been extensively studied for platinum nanoclusters (0-D nanostructures) [25-29]. Nevertheless, the causes that restricted the formation of metal nanostructures such as nanowires, networks, and nanoflowers were unreported at the start of this research project.

Among the most recent and relevant results regarding the formation of metal nanowires using zeolites, it was found that Zhou et al. achieved the synthesis of silver nanowires from LTA zeolite with a transmission electron microscope [30, 31]. The silver nanowires were generated outside of the zeolite and had diameters in a range of 20 to 50 nm. The mechanism was described by Zhou et al. as an extrusion process, in which the Ag^{+} cations inside of the template migrated toward the external sector of the zeolite in order to be reduced with the electron beam ($Ag^{+} + e^{-} \rightarrow Ag^{0}$). It is known that in a reduction process the cationic species migrate toward sectors where

there is a high density of electrons due to the electric field generated. It is highlighted that in this work the zeolite did not work as template and that the migration was induced by the electron sources.

The work in this dissertation has helped identify some critical parameters that enable the synthesis of nanowires in zeolites and as a result an effective synthesis protocol was developed by solid state reduction.

1.1 Porous materials

The term “porous material” is usually related to solid materials integrated of void spaces or cavities in their structures. They can be classified according to International Union of Pure and Applied Chemistry (IUPAC) by the pore diameter or aperture size. Porous materials with pore diameters of 2 nm or less are classified as microporous. Mesoporous materials is the name given to materials with pore sizes in the range of 2 nm to 50 nm. Materials containing pores with diameters over 50 nm are known as macroporous. The porosity dramatically impacts the performance of the materials for application in catalysis and gas adsorption [32]. Since this dissertation is mainly focused on the use of zeolites a detailed description of them follows.

1.1.1 Zeolites

Zeolites are crystalline materials that are found in nature, in mines, volcanic zones, and can be also synthesized in laboratories. The term zeolite was

proposed by a mineralogist and chemist named Axel Fredrik Cronstedt in the year 1756. The word zeolite is derived from the Greek words ζέω (*zeō*) y λίθος (*lithos*), whose translations are 'to boil' and "stone," respectively, due to the fact that when this material was heated a large amount of vapors emerged [24].

The pore diameters of zeolites range between 0.4 and 0.8 nm. they are frequently used as sieves at the molecular scale, restraining the passage of molecules of large sizes [24].

Zeolites are, in general, composed of tetrahedrally coordinated Si-O and Al-O. The presence of the Al^{+3} atoms in the structure generates a negative charge that is compensated with an extra-framework cation. The presence of these cations have made zeolites useful for ion exchange, catalytic, and adsorption applications [24]. The Si/Al ratio varies in zeolites from 1 to infinity where infinity is for pure silica zeolites. According to the Lowenstein's rule, a zeolite with a ratio of silicon/aluminum lower than 1 is difficult due to the electrostatic repulsion between the adjacent tetrahedrally coordinated aluminum atoms that make formation of Al-O-Al bonds unfavorable energetically [24]. A summary of how the properties of the aluminosilicate zeolites change with increasing Si/Al ratio is presented in the Table 1.1.

In general, the chemical formula of a zeolite can be expressed as follows:

$$|A_{x/n}M_m|\ [Al_xSi_yO_{2(x+y)}] - \text{IZA} \qquad 1.1$$

Where $|A_{x/n}M_m|$ represents chemical species incorporated into the structure of the zeolite and the term $[Al_xSi_yO_{2(x+y)}]$ describes the composition of the framework. *A* is the extraframework cation, *M* is a guest molecule, *n* is the valency of the cation, and *x* ,*y*, and *m* represent the number of moles of Al, Si, and the guest molecules (commonly water). The term IZA is associated with the three letters used as a code to identify the framework type [24].

Table 1.1 Variation of zeolite properties as Si/Al ratio increases.

Property	Si/Al ratio of 1 to ∞
Stability	From ≤ 700 °C to ~ 1300 °C
Surface selectivity	Hydrophilic to hydrophobic
Cations concentrations	Decreasing

Aluminophosphates are microporous materials with alternating tetrahedrally coordinated Al-O and P-O atoms. The structures are similar to zeolites where the silicon atoms (Si^{4+}) are replaced with phosphorus atoms. Due to their similarity they are considered zeolitic materials as well. The tetrahedral coordination of the P^{5+} generates a positive charge in the structure that is compensated with the negative charge generated by the Al^{+3} tetrahedra. When there is a strict P-O-Al-O

ordering in the structure, no extra-framework cations are needed to balance the structure [24].

In this dissertation the formation of platinum nanostructures was evaluated in zeolites ECR-5, mordenite, and VPI-5. All these zeolites have one dimensional pore channels. The main pore channel size of ECR-5 (CAN) is of 0.54 nm with a window of 12 tetrahedral atoms (T-atoms) and space group is $P6_3/mmc$. This zeolite was synthesized with a ratio of Si/Al approximately of 1.3. Mordenite (MOR) had a main pore size of 0.65 nm containing12 T-atoms,and space group Cmcm. The molar ratio of Si/Al in the mordenite used was approximately 6.5. (Figure 1.1). VPI-5 (VFI) is an aluminophosphate that has a Al/P= 1 and a completely neutral framework. Its main pore size is 1.2 nm and its space group is $P6_3/mcm$. VPI-5 was used because of its relatively large pores to reduce the resistance of the platinum precursor to migrate inside of the zeolites [24]. It was the first molecular sieve synthesized with ultra wide pores and it was discovered by Davis et al. in 1988.

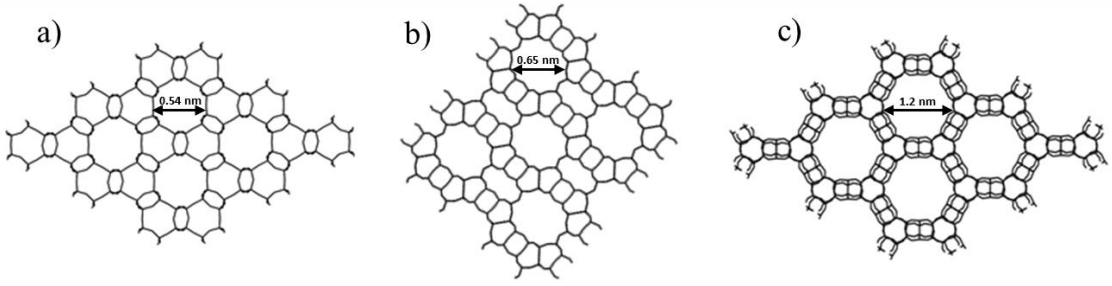

Figure 1.1 Structures of a) ECR-5 (CAN), b) Mordenite (MOR), and c) VPI-5 (VFI).

1.1.2 Zeolite synthesis

Near the year 1950, the first synthesis methods to obtain zeolites that occurred naturally in mines were developed. This favored an accelerated growth of the market of zeolites for commercial applications. Despite the fact that natural zeolites had been identified since 1756, they did not have a significant importance at the industrial level due to their variations in crystallinity, purity and pores. Therefore, zeolites used commercially are generally synthesized in laboratories [24].

Hydrothermal synthetic techniques are the most common methods for the formation of zeolites. These techniques are focused on the employment of high temperatures (>100 °C) and pressures (1 bar) reaction conditions in a closed system.

The synthesis of zeolites can be generally summarized in three steps. The first step requires the preparation of an aqueous super saturated solution with the appropriate concentration of the structure directing agent, aluminum atoms and silicon atoms, creating a gel-like solution [24].

The role of the structure directing agent is generating an appropriate crystallization of the zeolite structure. Among the most used are tetrapropylammonium hydroxide (TPAOH), tetraethylammonium hydroxide (TEAOH) and tetrabutylammonium hydroxide (TBAOH). Other important reactants that affect the crystallization of the zeolite are the sources of aluminum and silicon atoms. Pseudoboehmite, sodium aluminate and aluminum hydroxide are some of the aluminum sources normally employed, while the most common silicon sources are

colloidal silica sol, tetramethylorthosilicate, and tetraethylorthosilicates. The concentration of the reactants is critical in the crystallization of the zeolite. As zeolites are metastable phases small changes in concentration can alter the growth of the desired zeolite.

The second step is loading the solution into a recipient (e.g. Teflon autoclave). The recipients are designed to support the high autogenic pressure built up during the synthesis process. The last step is the heating; the recipient is located generally in a convective oven at a synthesis temperature between 100 and 250 °C [24].

Aluminophosphates are typically synthesized hydrothermally as well. The source of phosphorus generally is *o*-phosphoric acid, while there are more options of aluminum sources such as pseudoboehmite and aluminum isopropoxide. The structure direct agent is generally an amine or a quaternary ammonium salt [24].

1.1.2.1 Synthesis of the aluminosilicate ECR-5.

The ECR-5 zeolite used in this work was synthesized based on [33] with a Si/Al ratio of 1.3. The procedure consisted in dissolving 12 g of NaOH and 28.4 g of LiOH in 218 g of deionized water. Then 36.2 g of HS-40 colloidal silica (DuPont Co.) and 55.3 g meta-kaolin were added to the solution to form a slurry. The composition of the slurry was:

$$1.2\ Li_2O{:}0.8Na_2O{:}Al_2O_3{:}3SiO_2{:}60H_2O$$

The reaction was carried out in a Teflon-lined stainless steel autoclave at a temperature of 120 °C for 72 hours.

1.1.2.2 Synthesis of VPI-5

The synthesis method of the zeolite VPI-5 used in this investigation was carried out following the steps described by N.Venkatathri [34]. Pseudoboehmite (3.58 g), kindly donated by SASOL, was mixed with 10 ml of distilled water. Then 5.75 g of ortho phosphoric acid (85% solution) was added dropwise to the mixture. The viscous white mixture was aged overnight at room temperature. After that, 2.969 g of di-*n*-propylamine (98%, Aldrich) mixed with 10 ml of deionizated water was added dropwise to the white paste. The mixture was stirred again for 10 min. The final mix was charged into a Teflon-lined stainless steel autoclave. The crystallization was carried out under rotation for 8 hours at 142 °C.

1.1.2.3 Synthesis of mordenite

The standard procedure for the synthesis of the zeolite mordenite [35], consists of dissolving 4.75 g NaOH in 10 g water. Then 3.575 g of sodium aluminate is added and stirred at 350 rpm until the dissolution of all the reactants is obtained. Following that step 161.25 g of H_2O are added followed by 24.55 g of SiO_2. This mixture is stirred at 350 rpm during 30 min. The gel prepared has a final composition

of: $6Na_2O:Al_2O_3:30.SiO_2:780.H_2O$. The mixture is then placed in a Teflon-lined stainless steel autoclave and the reaction is carried out during a period of 36 hours [35].

After synthesis of the desired zeolites, the focus of the research was on developing methods of synthesis of nanostructures inside their pores. Below is an introduction of how this is generally done but the actual techniques used and the results are discussed in the chapters 3, 4, and 5.

1.2 Incorporation methods

In the process of incorporating precursors to a support for the formation of templated nanostructures the walls of the support can interact with the precursor via hydrogen bonding, Coulomb interactions and Van der Waals forces. These interactions contribute to the migration of the precursor inside of the support [36]. This section discusses common techniques used to incorporate platinum precursors in supports, namely wet impregnation and incipient wetness impregnation.

The wet impregnation method consists on dispersing the template in an aqueous solution of the metal precursor. In a typical process the solution is stirred during a determinate period of time. In this technique the amount of precursor incorporated in the support is limited by the capacity of adsorption of the material [36].

In this technique there are no strong interactions between the precursor and the walls of the support. The template loaded with the precursor may be recovered using extraction methods such as filtration or evaporation. When evaporation is used,

the amount of platinum precursor in the support can be approximated. When the recovery of the support is done using filtration, the amount of the precursor must be measured [36].

When wet impregnation is done at higher temperatures (70 °C to 90 °C) and the recovery is by filtration, the incorporation is considered to occur by ion exchange. The ion exchange method is based on the interchange of cations in the support by the positively charged metal precursors. This technique ensures a strong interaction between the support and the metal precursor. In the ion exchange method the amount of metal incorporated is restrained by the ion exchange capacity of the zeolite [37].

The incipient wetness impregnation method typically consists of adding an aqueous solution with a predetermined amount of the metal precursor drop by drop to the support until its available pore volume fills up. The metal precursor diffuses through the pores through capillary action. Because there is no excess of solution this method does not require filtration. This method is used to ensure that the platinum precursor is deposited on the internal pores of the support (as opposed to on the surface), to control the amount of metal deposited and to have a higher loading than what is achievable through ion exchange [36].

1.3 Reducing agents

Reducing agents are chemical species that reduce other compounds in reduction –oxidation (red-ox) reactions. They are the oxidized chemical species by donating their electrons. A red-ox process can be expressed in general way with the Equations 1.6 and 1.7 below:

$$X^m \rightarrow ne^- + X^{m-n} \quad \textbf{1.2}$$

$$M^{n+} + ne^- \rightarrow M^0 \quad \textbf{1.3}$$

In Equation 1.6, the X^m is the reducing agent that donates n electrons (ne^-), and is oxidized to X^{m-n}. The specie M^{n+} in Equation 1.7 is reduced to M^0 by the incorporation of the electrons (ne^-). Stronger reducing agents are those who give their electrons more easily. Atoms or chemical species which have a lower electronegativity tend to be better reducing agents, because the electronegativity is a measure of the strength with which the atoms (molecules or functional groups) attract electrons [37].

Chemical species that have a relatively large atomic radius tend to be better reducing agents, due to that the great distance from the nucleus to the electrons allows them to be easily expelled. The oxidation potential of a reducing agent and its ability to reduce other compounds is determined by the standard reduction potential (E^o). This value is referred to as the potential (V) required to remove electrons of the chemical specie at standard conditions of 25 °C of temperature, 1 mol/L concentration of and 1 bar of pressure (for gases) [37].

The higher negative values of E^o indicate that the reducing agent has a great capacity to donate electrons and reduce other chemical species, while positive values of E^o mean that the reducing agent has difficulty donating electrons at standard conditions. The reduction potential of the reducing agents at nonstandard conditions is calculated using the Nerst equation [37]. The Nerst equation is described in the Equation 1.8:

$$E_{red.Agent.} \equiv E^{\circ} - \frac{RT}{nF} \ln Q \qquad \textbf{1.4}$$

Where, Q is the relation of X^m/X^{m-n}. Equation 1.8 indicates that the reducing potential rises with the increasing of the temperature and concentration of the reducing agent. Some reducing agents used in the literature for synthesis of metal nanowires are: methanol, ethylene glycol, formic acid, sodium borohydride and hydrogen gas [1-3, 20, 21].

Table 1.2 Standard reduction potential E^o,(V) of some reducing agent used for the synthesis of nanostructures.

Reducing agent	**E^o, (V)**
Sodium borohydride	-1.24
Hydrogen	0
Methanol	0.13

1.4 References

[1] Chen A, Holt-Hindle P (2010) Platinum-Based Nanostructured Materials: Synthesis, Properties, and Applications. Chemical Reviews 110:3767-3804

[2] Teng X, Yang H (2005) Synthesis of Platinum Multipods: An Induced Anisotropic Growth. Nano Letters 5:885-891

[3] Song Y, Garcia RM, Dorin RM, Wang H, Qiu Y, Coker EN, Steen WA, Miller JE, Shelnut JA (2007) Synthesis of platinum nanowire networks using a soft template. Nano Letters 7:3650-3655

[4] Sasaki M, Osada M, Higashimoto N, Yamamoto T, Fukuoka A, Ichikawa M (1999) Templating fabrication of platinum nanoparticles and nanowires using the confined mesoporous channels of FSM-16--their structural characterization and catalytic performances in water gas shift reaction. Journal of Molecular Catalysis A: Chemical 141:223-240

[5] Hrapovic S, Liu Y, Male KB, Luong JHT (2003) Electrochemical Biosensing Platforms Using Platinum Nanoparticles and Carbon Nanotubes. Analytical Chemistry 76:1083-1088

[6] Panyam J, Labhasetwar V (2004) Sustained Cytoplasmic Delivery of Drugs with Intracellular Receptors Using Biodegradable Nanoparticles. Molecular Pharmaceutics 1:77-84

[7] Collins L, Kaszuba M, Fabre JW (2004) Imaging in solution of (Lys)16-containing bifunctional synthetic peptide/DNA nanoparticles for gene delivery. Biochimica et Biophysica Acta (BBA) - General Subjects 1672:12-20

[8] Zharov VP, Letfullin RR, Galitovskaya EN (2005) Microbubbles-overlapping mode for laser killing of cancer cells with absorbing nanoparticle clusters. Journal of Physics D: Applied Physics 38:2571-2581

[9] Yong Z, Nathan K, Miqin Z (2002) Surface modification of superparamagnetic magnetite nanoparticles and their intracellular uptake. Biomaterials 23:1553-1561

[10] Scott RWJ, Wilson OM, Crooks RM (2005) Synthesis, Characterization, and Applications of Dendrimer-Encapsulated Nanoparticles. The Journal of Physical Chemistry B 109:692-704

[11] Moser A, Takano K, Margulies DT, Albrecht M, Snobe Y, Ikeda Y, Sun S, Fullerton E (2002) Magnetic recording: advancing into the future. Journal of Physics D: Applied Physics 35:157-167

[12] Xia Y, Yang P (2003) Chemistry and physics of nanowires. Advanced Materials 15:351-352

[13] Fukuoka A, Sakamoto Y, Higuchi T, Shimomura N, Ichikawa M (2006) Synthesis and electronic property of platinum nanowire and nanoparticle in mesoporous silica template. Journal of Porous Materials 13:231-235

[14] Chen H, Yuan R, Chai Y, Wang J, Li W (2010) Glucose biosensor based on electrodeposited platinum nanoparticles and three-dimensional porous chitosan membranes. Biotechnology Letters 32:1401-1404

[15] Yang M, Qu F, Lu Y, He Y, Shen G, Yu R (2006) Platinum nanowire nanoelectrode array for the fabrication of biosensors. Biomaterials 27:5944-5950

[16] Fengli Q, Minghui Y, Guoli S, Ruqin Y (2007) Electrochemical biosensing utilizing synergic action of carbon nanotubes and platinum nanowires prepared by template synthesis. Biosensors and Bioelectronics 22:1749-1755

[17] Araki H, Fukuoka A, Sakamoto Y, Inagaki S, Sugimoto N, Fukushima Y, Ichikawa M (2003) Template synthesis and characterization of gold nano-wires and -particles in mesoporous channels of FSM-16. Journal of Molecular Catalysis A: Chemical 199:95-102

[18] Fukuoka A, Higashimoto N, Sakamoto Y, Inagaki S, Fukushima Y, Ichikawa M (2002) Preparation, XAFS Characterization, and Catalysis of Platinum Nanowires and Nanoparticles in Mesoporous Silica FSM-16. Topics in Catalysis 18:73-78

[19] Fukuoka A, Higashimoto N, Sakamoto Y, Sasaki M, Sugimoto N, Inagaki S, Fukushima Y, Ichikawa M (2001) Ship-in-bottle synthesis and catalytic performances of platinum carbonyl clusters, nanowires, and nanoparticles in micro- and mesoporous materials. Catalysis Today 66:23-31

[20] Fukuoka A, Higuchi T, Ohtake T, Oshio T, Kimura J-i, Sakamoto Y, Shimomura N, Inagaki S, Ichikawa M (2006) Nanonecklaces of Platinum and Gold

with High Aspect Ratios Synthesized in Mesoporous Organosilica Templates by Wet Hydrogen Reduction. Chemistry of Materials 18:337-343

[21] Sakamoto Y, Fukuoka A, Higuchi T, Shimomura N, Inagaki S, Ichikawa M (2003) Synthesis of Platinum Nanowires in Organica Inorganic Mesoporous Silica Templates by Photoreduction: Formation Mechanism and Isolation. Journal of Physical Chemistry B 108:853-858

[22] Yang C-M, Sheu H-S, Chao K-J (2002) Templated Synthesis and Structural Study of Densely Packed Metal Nanostructures in MCM-41 and MCM-48. Advanced Functional Materials 12:143-148

[23] Liu Z, Terasaki O, Ohsuna T, Hiraga K, Shin HJ, Ryoo R, Liu Z (2001) An HREM Study of Channel Structures in Mesoporous Silica SBA-15 and Platinum Wires Produced in the Channels. ChemPhysChem 2:229-231

[24] Van Bekkum H, Flanigen E M, Jacobs P A, Jansen J C (2001) Studies in surface science and catalysis 137. Elsevier science, Amsterdam

[25] Yang Y-X, Bourgeois L, Zhao C, Zhao D, Chaffee A, Webley PA (2009) Ordered micro-porous carbon molecular sieves containing well-dispersed platinum nanoparticles for hydrogen storage. Microporous and Mesoporous Materials 119:39-46

[26] Van de Vyver S, D'Hondt E, Sels B, Jacobs P, Gaigneaux E, Devillers M, Hermans S, Jacobs P, Martens J, Ruiz P (2010) Preparation of Pt on NaY zeolite

catalysts for conversion of glycerol into 1,2-propanediol. In: Studies in Surface Science and Catalysis Elsevier, pp. 771-774

[27] Chakarova K, Hadjiivanov K, Atanasova G, Tenchev K (2007) Effect of preparation technique on the properties of platinum in NaY zeolite: A study by FTIR spectroscopy of adsorbed CO. Journal of Molecular Catalysis A: Chemical 264:270-279

[28] de Graaf J, van Dillen AJ, de Jong KP, Koningsberger DC (2001) Preparation of Highly Dispersed Pt Particles in Zeolite Y with a Narrow Particle Size Distribution: Characterization by Hydrogen Chemisorption, TEM, EXAFS Spectroscopy, and Particle Modeling. Journal of Catalysis 203:307-321

[29] Ismagilov ZR, Yashnik SA, Startsev AN, Boronin AI, Stadnichenko AI, Kriventsov VV, Kasztelan S, Guillaume D, Makkee M, Moulijn JA (2009) Deep desulphurization of diesel fuels on bifunctional monolithic nanostructured Pt-zeolite catalysts. Catalysis Today 144:235-250

[30] Zhou W, Edmondson M, Anderson P, Edwards P (2001) TEM studies of the in-situ growth of silver metal nanowires from zeolites. Electron Microscopy and Analysis 168:397-400

[31] Yuan Z-Y, Zhou W, Parvulescu V, Su B-L (2003) Electron beam irradiation effect on nanostructured molecular sieve catalysts. Journal of Electron Spectroscopy and Related Phenomena 129:189-194

[32] Webb P, Orr C, Camp R, Olivier J, Yunes Y (1997) Analytical Methods in Fine Particle Technology. Micromeritics Instrument Corporation, USA

[33] Vaughan D (1991) Process for preparation of an ECR-5 crystalline zeolite composition. US Patent 5015454, USA.

[34] Venkatathri N (2003) An improved process for the synthesis of VPI-5 molecular sieve. Bull. Mater. Sci. 26:279-281

[35] Mignoni ML, Petkowicz DI, Fernandes Machado NRC, Pergher SBC (2008) Synthesis of mordenite using kaolin as Si and Al source. Applied Clay Science 41:99-104

[36] Tiemann M (2007) Repeated Templating. Chemistry of Materials 20:961-971

[37] Fundamentals of electrochemical deposition, New York, A Wiley Inter-Science, 1998.

Chapter 2 SYNTHESIS OF SUPPORTED PT NANOPARTICLES, MULTIPODS, NANOFLOWERS, AND NANOWIRES IN ZEOLITE MORDENITE BY VARYING THE METAL PRECURSOR AND THE REDUCTION METHODS

Abstract

Pt nanostructures have been studied for applications that range from fuel cell catalysts to sensors and they have been synthesized through a myriad of template and templateless methods. Here the effect of the metal precursor charge and reduction methods when using zeolite mordenite is explored. It was observed that H_2PtCl_6 has a natural tendency to form anisotropic Pt structures on the surface of the zeolite regardless of the reduction method, while $Pt(NH_3)_4(NO_3)_2$ promoted the formation of diverse Pt nanostructures inside the pores of the zeolite. It was also observed that the more condensed the reducing agent the more anisotropic the resulting Pt nanostructures were. The formation of Pt structures that include well dispersed nanoclusters, multipods, nanoflowers and nanowires is reported.

2.1 Introduction

Platinum nanostructures are very attractive due to the physical and chemical properties they exhibit as a function of size, shape, and crystalline configuration [1]. They are being widely studied for integration into devices such as fuel cells and biosensors [1, 2].

As an example, platinum nanocluster modified electrodes have shown good sensitivity and stability for the detection of glucose, hydrogen peroxide and DNA [3-6]. Meanwhile, platinum nanowires arranged in a nanoelectrode assembly have been shown to provide sensitivity for the detection of peroxide that is 50 times higher, when compared to conventional platinum disk electrode [7].

Platinum nanowires are some of the most interesting and promising nanostructures because, due to their morphology, they can exhibit quantum confinement effects of electrons axially [1]. Further development of Pt nanowires could potentially enable novel applications in fields such as catalysis, gas absorption, and electron transport [2, 8].

The template method has proven to be an efficient bottom-up approach to synthesizing small platinum nanostructures [9-14]. There are two main synthetic routes to generate templated platinum nanostructures: using hard templates and soft templates. The hard template route is focused on the reduction of the metal inside a solid porous matrix, while the soft template is associated with the reduction of the metal in the presence of a capping surfactant or organic solvent.

As stated in Chapter 1 solid porous templates can be classified according to their pore size in microporous, mesoporous, and macroporous materials [1, 11] [15]. Articles on the synthesis of Pt nanoparticles using porous tamplates abound. In macroporous materials such as anodic aluminum oxide (AAO), platinum nanoparticles, nanotubes and nanowires have been synthesized by reduction of the metal with, for example, sodium borohydride and by electrochemical deposition [3, 13, 16]. In mesoporous silicas, metal nanoclusters are usually synthesized by thermal reduction with hydrogen gas [12, 17-22], while metal nanowires have been synthesized using less traditional reduction methods, such as water saturated hydrogen in hierarchically ordered mesocellular mesoporous silica (HMM) [20], photo-reduction with methanol using UV light in HMM-1 [12], and sodium borohydride in solution in mesoporous silica MCM-41 [10].

Using soft templates, Chen and co-workers [23] reported the synthesis of single crystal "sea urchin" platinum nanowires, using a polyol process at 110 °C, H_2PtCl_6 as the platinum precursor and ethylene glycol as a reducing agent. In this study temperature was a critical parameter to obtain the nanostructures, as no Pt nanoparticles formed at room T. Similarly, Herrichs and coworkers [24] obtained morphological control over platinum nanostructures using H_2PtCl_6 as a precursor and ethylene glycol as a reducing agent. In this study the reduction of the precursor was controlled with $NaNO_3$ at room temperature. When the molar ratio between $NaNO_3$ and H_2PtCl_6 was increased from 0 to 11, the morphology of the platinum

nanostructures changed from spheroidal particles toward more irregular structures (tetrahedral o octahedral), presumably due to the slowing of the reduction reaction.

An alternative synthetic route that was template- and surfactant- free was developed by Sun S. et al. to obtain platinum nanoflowers. In this synthesis method H_2PtCl_6 was mixed with an aqueous solution of formic acid at room temperature and at atmospheric pressures for up to 16 hours. When the synthesis was done at higher temperatures (50 °C and 80 °C), the formation of nanoparticles was favored, as the reduction was much faster than at room temperature [25].

These studies show that when the rate of reduction is lowered without being suppressed, the formation of anisotropic nanostructures is preferred by becoming a Pt diffusion dominated process [14, 23-26].

In microporous materials, on the other hand, even though synthesis of platinum nanoclusters has been well studied for catalytic applications [27, 28], the development of synthesis methods to obtain anisotropic platinum nanostructures remains a challenge today. In a previous article, our research group reported the formation of platinum nanowires with a diameter of 6.57 nm inside the pores of the zeolite mordenite using the precursor $Pt(NH_3)_4(NO_3)_2$ and using $NaBH_4$ in the solid state as a reducing agent [29]. This article evaluated the $NaBH_4$:Pt ratio required for the formation of platinum nanowires. Zeolite mordenite was chosen for that particular study and also here because it has 1D pore channel structures that could promote the formation of nanowires and because it has a high concentration of tetrahedrally

coordinated alumina which could promote the even dispersion of positively charged Pt precursors. In fact, one of the factors studied in this article is how the platinum precursor charge affects the formation of the Pt nanoparticles in zeolites.

In general, this article explores how non-traditional reduction methods that have been successful in the formation of Pt nanowires in other systems affect the structure of the Pt when using zeolite mordenite as a template. The result is a wide range of nanostructures: nanoparticles, nanoflowers, multipods and nanowires. While discussing the results this article aims to explain why the solid state reduction method is necessary for the formation of Pt nanowires in zeolites.

2.2 Chemicals and Materials

Na-Mordenite (CBV-12A) with a Si/Al = 6.5 was purchased from the company Zeolyst International. Chloro platinic acid hydrate ($H_2PtCl_6 \cdot H_2O$) and tetraamineplatinum (II) nitrate ($Pt(NH_3)_4(NO_3)_2$) were obtained from Alfa Aesar/Johnson Matthey. Ultra high purity gas Nitrogen (N_2, 99.9999 % pure) and hydrogen (H_2, 99.9999 % pure) were obtained from Linde Gas. Ethylene glycol ($HOCH_2CH_2OH$) and methanol (CH_3OH, 99.8 %) were acquired from Fisher chemical (USA). Formic acid (ACS, 96+ %) and potassium borohydride (KBH_4 , 98 %) were obtained from Alfa Aesar company.

2.3 Experimental Section

Zeolite mordenite was pretreated in vacuum (10 μmHg) at 400°C for a period of 12 hours to remove any impurities present in their pores. Pretreated 200 mg mordenite samples were then impregnated with the aqueous solution of $PtCl_6^{2-}$ and $Pt(NH_3)_4^{2+}$ via incipient wetness impregnation to achieve a platinum concentration of 5% wt. Samples impregnated with both the negative and positive precursors were then reduced with the six methods described below.

In reduction method A, the samples were placed into a tubular reactor on a ceramic boat, where the samples were heated at a temperature ramp rate of 2.91 °C/min under H_2 gas (50 mL/min, 99.999 %) from 25 °C to 200 °C, and maintained at 200 °C for 2 hours. Then the samples were cooled under nitrogen gas (50 mL/min, 99.9999 %). The samples were heated at a temperature of 200 °C to induce the complete thermal reduction of the metal precursor. These are the conditions optimized by Fukuoka et al. in mesoporous silicas [20].

Also following the work by Fukuoka and coworkers [20], in reduction method B, the samples were placed into a tubular reactor on a ceramic boat where the samples were heated at a temperature ramp of 2.91°C/min under hydrogen gas saturated with water vapor (H_2, 50 mL/min, 99.999 %) from 25 °C to 200 °C, and maintained at 200 °C for 2 hours. Later, the samples were cooled under nitrogen gas (50 mL/min, 99.9999 %).

Reduction method C was inspired by the work of Sun et al. [25] in template-less systems and it consisted of adding formic acid (50 µl) drop by drop onto the samples of Pt/MOR. The reactions were carried out at room temperature for 48 hours, where the samples were mixed in intervals of 8 hours until they achieved the gray color characteristic of reduced platinum. The same reduction method was done at 110 °C for comparison and is denoted as C'.

In reduction method D, ethylene glycol was used as a reducing agent. The procedure consisted of adding ethylene glycol (50 µl) drop by drop onto the samples (Pt/MOR) at room temperature. After adding ethylene glycol, the samples were placed in an isothermal furnace at a controlled temperature of 110 °C for 48 hours where the samples were stirred for a short period of time every 8 hours. The temperature in this case was raised to 110 °C following the work by Chen [23]. The same reduction method was also done at 200 °C and is denoted as D'.

Following the reduction method described by Sakamoto et al. [30], in reduction method E the samples were impregnated with 50 µl of methanol and put under vacuum for 2 hours. Then the samples were exposed to UV light for 48 hours and were stirred at intervals of 4 hours until they achieved a gray color.

In the final method F, the samples of Pt/MOR were thoroughly mixed with potassium borohydride powder (KBH_4) using the procedure described in Chapter 3 using a 10:1 KBH_4:Pt ratio [29]. The reduction methods are summarized in Table 2.1.

Table 2.1 Description of experimental synthesis conditions

Reduction Method	Platinum precursor	Reducing agent and experimental conditions
A	$Pt(NH_3)_4^{2+}$	H_2 gas at 200 °C for 2 hours
	$PtCl_6^{2-}$	
B	$Pt(NH_3)_4^{2+}$	Hydrogen gas saturated with water vapor at 200 °C for 2 hours
	$PtCl_6^{2-}$	
C	$Pt(NH_3)_4^{2+}$	Formic acid at room temperature for 48 hours
	$PtCl_6^{2-}$	
C’	$Pt(NH_3)_4^{2+}$	Formic acid at 110 °C temperature for 48 hours
	$PtCl_6^{2-}$	
D	$Pt(NH_3)_4^{2+}$	Ethylene glycol at 110 °C for 48 hours
	$PtCl_6^{2-}$	
D’	$Pt(NH_3)_4^{2+}$	Ethylene glycol at 200 °C for 48 hours
	$PtCl_6^{2-}$	
E	$Pt(NH_3)_4^{2+}$	Methanol and put under vacuum and UV light for 48 hour
	$PtCl_6^{2-}$	
F	$Pt(NH_3)_4^{2+}$	Potassium borohydride at room temperature for 48 hours
	$PtCl_6^{2-}$	

2.4 Characterization

The morphology of the platinum nanostructures was characterized by transmission electron microscopy (TEM) using a Carl Zeiss Leo 922. The sample preparation for TEM analysis consisted of suspending the sample in isopropanol and applying vibration for 1 min. A 17 μL drop of the solution was added to an ultrathin carbon grid which was dried at room temperature.

2.5 Results and Discussion

Figure 2.1(a) shows that platinum nanoparticles were formed on the surface of mordenite (MOR) when the $PtCl_6^{2-}$/MOR sample was reduced with method

A. The nanoparticles have an average size of 77 nm (StDev = 3 nm) and have a solid core but also have a rough surface that suggest that nanowire-like structures have formed on it. On the other hand, Figure 2.1(b) shows that well dispersed platinum nanoclusters are formed inside mordenite when using $Pt(NH_3)_4^{2+}$ and the same reduction method. The nanoclusters have an average diameter of 3.9 nm (StDev = 1 nm), a typically reported size for platinum nanoclusters formed inside zeolites [31, 32]. Nanoclusters are differentiated from nanoparticles by their size, nanoclusters are those nanoparticles that are less than 10 nm in diameter.

These two TEM images suggest that the negatively charged precursor had difficulty incorporating into the zeolite while the positively charged was able to incorporate easily. This is probably due to repulsion of the negatively charged mordenite structure. The tendency for the formation of nanostructures on the surface of the zeolite when using $PtCl_6^{2-}$ as a precursor was observed with the other reduction methods studied as well. As a consequence, in general, the nanostructures formed using $PtCl_6^{2-}$ grew to form larger particles. a result that is similar to that found by Rivallan et al. [33].

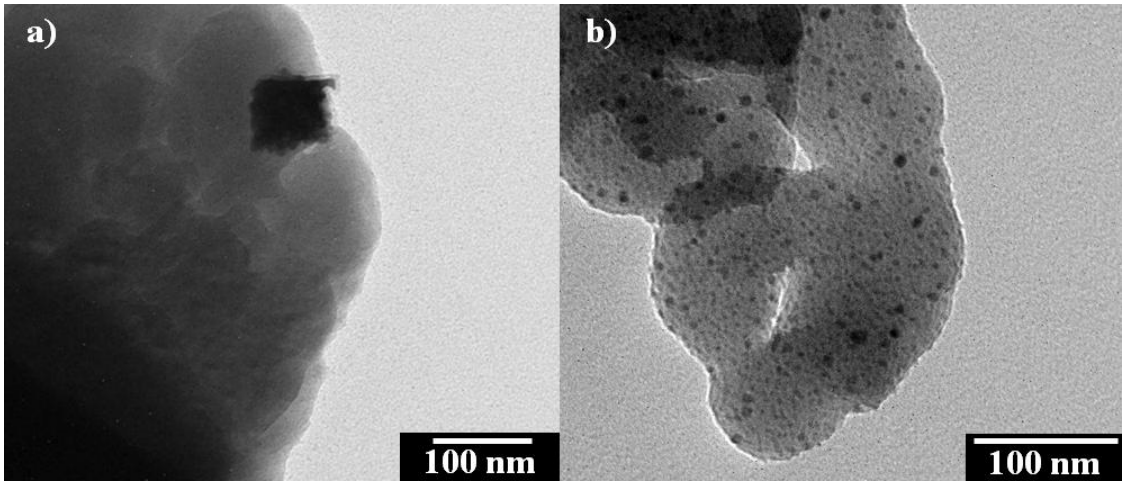

Figure 2.1 Bright field TEM images of (a) platinum nanoparticles with nanowire-like structures on its surface obtained in $PtCl_6^{2-}$/MOR and (b) platinum nanoclusters formed in $Pt(NH_3)_4^{2+}$/MOR by H_2-reduction.

TEM images of platinum nanostructures that were formed by reduction method B are shown in Figure 2.2. Figure 2.2(a) shows that for the $PtCl_6^{2-}$/MOR sample, platinum nanoflower like structures are formed on the surface of the zeolite. The nanostructures had an average core diameter of 81 nm (StDev = 15 nm) surrounded by nanowires approximately 33 nm in length and 5 nm in diameter. When compared to the results by Fukuoka [20] who used this same precursor and reducing protocol the same tendency to form anisotropic nanostructures is observed with the evident difference that in mordenite they are formed on the surface of a core particle grown on the surface of the zeolite while in the mesoporous silicas the nanowires were formed inside the pores. Overall, these results suggest that the water in the hydrogen

promotes the diffusion of the Pt atoms from the $PtCl_6^{2-}$ to form elongated structures. This could be due to the affinity of this precursor with water that increases its mobility on the surface of the particle core.

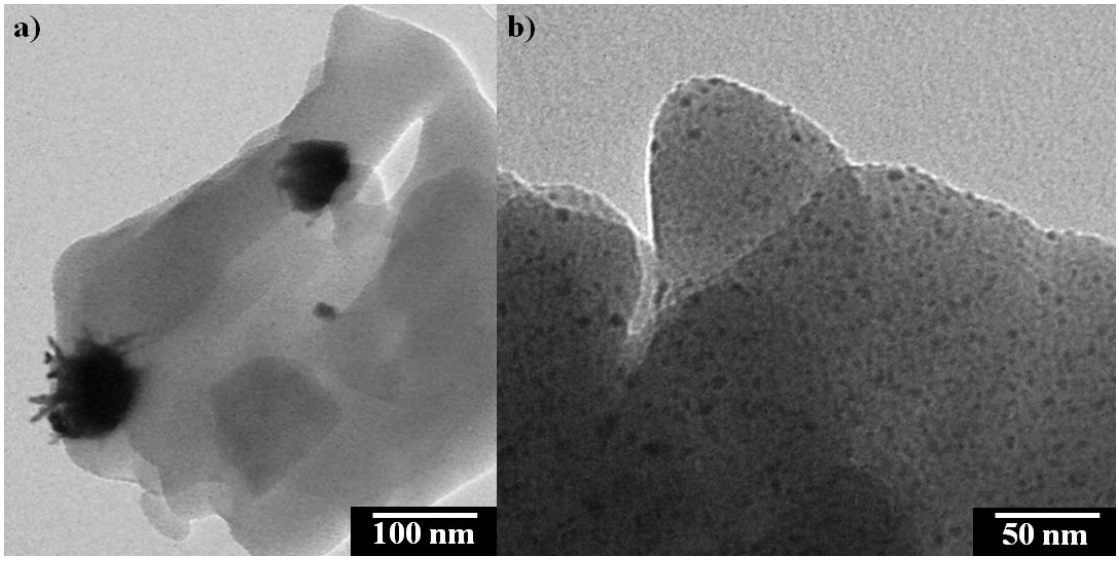

Figure 2.2 Bright field TEM images of (a) Platinum nanoflowers formed in $PtCl_6^{2-}$/MOR and (b) Pt nanoclusters formed in $Pt(NH_3)_4^{2+}$/MOR via reduction with H_2 saturated in water.

The $Pt(NH_3)_4^{2+}$/MOR sample reduced with method B yielded dispersed nanoclusters with an average size of 2.2 nm (StDev = 0.346 nm) as shown in Figure 2.2(b). These nanoclusters were smaller in size and more homogeneously distributed than those synthesized without the water saturation. The mechanism of this synthesis appears to be different than that using $PtCl_6^{2-}$ as a precursor and mesoporous silica as a template. Here the water molecules appear to either limit the diffusion of the Pt

particles or increase the reaction rate of the reduction process. One possible explanation is that the water that is known to preferentially adsorb in the small cavities of the zeolite works as a capping agent for the nanoclusters [34].

Figure 2.3(a) shows the growth of nanostructures in the surface of the zeolite mordenite of the $PtCl_6^{2-}$/MOR reduced with formic acid. As in Figure 2.2(a) these platinum structures appear to have nanowires growing from the surface of a spherical core. However, in contrast to Figure 2.2(a) these cores are denser. The platinum individual nanowires have approximate diameters of 4 nm and an average of 20 nm in length, while the average diameter of the nanoparticles core is 166 nm (StDev = 50 nm).

This result can be contrasted to the results reported by Sun S. et al. [25] where using this precursor without a template single crystalline platinum nanoflowers with 150-400 nm diameters and 100-200 nm in length nanowires were obtained. This suggests that the fact that the zeolite exists as a nucleation site tends to favor the formation of a larger core and smaller nanowires. Meanwhile, when comparing Figure 2.3(a) with Figure 2.2(a) and Figure 2.1(a) a general tendency can be observed towards the formation of anisotropic structures on the surface of spherical cores when using the $PtCl_6^{2-}$ in zeolite mordenite. This is a combination of the effects of the electrostatic repulsion of the precursor with the zeolite framework mentioned previously and the natural tendency of the $PtCl_6^{2-}$ to form anisotropic platinum nanostructures.

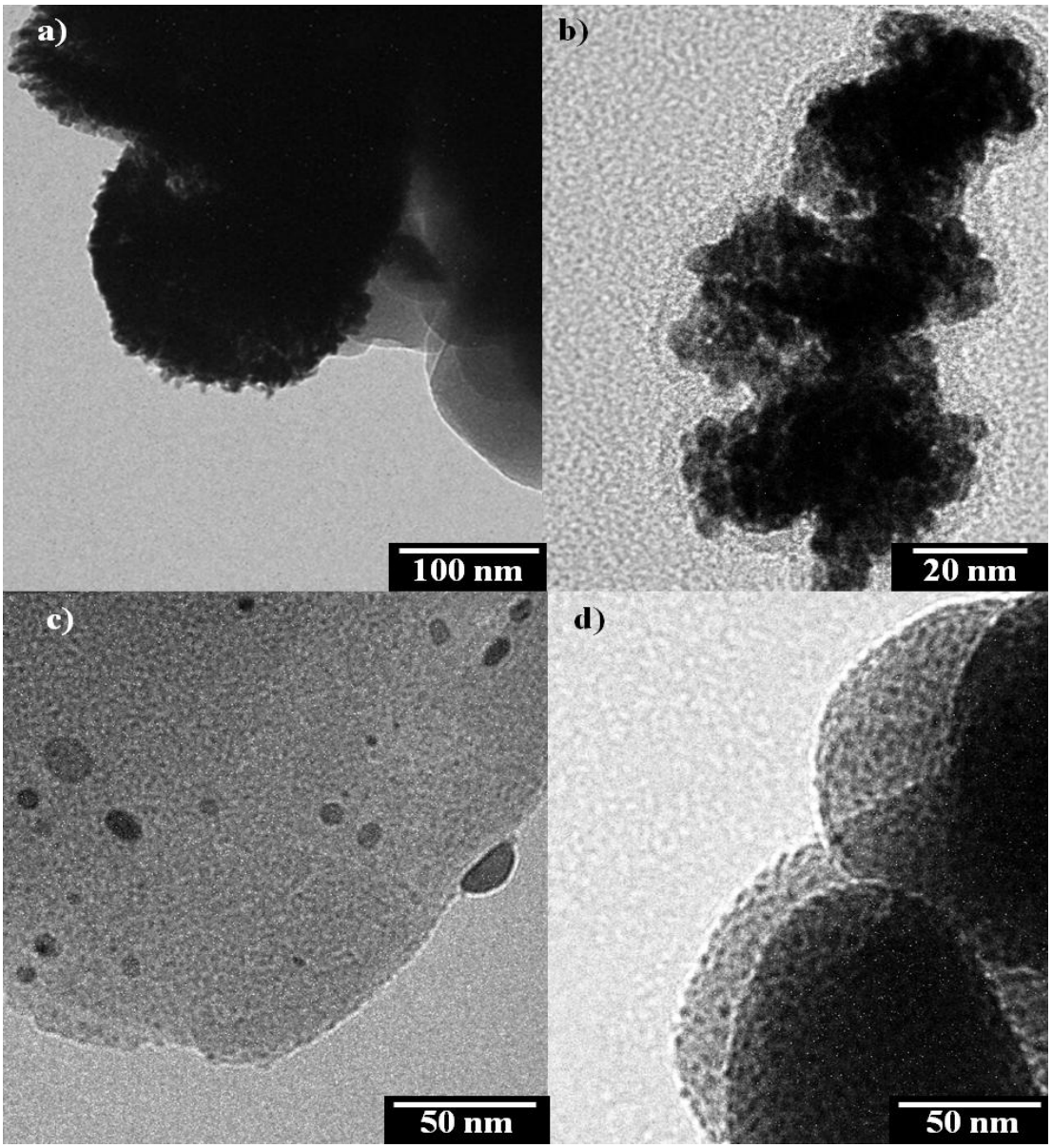

Figure 2.3 **Bright field TEM images of (a) platinum nanoparticles with nanowires on the surface and (b) agglomerated platinum nanoclusters, obtained after reduction of the $PtCl_6^{2-}$/MOR and $Pt(NH_3)_4^{2+}$/MOR samples, using formic acid as reducing agent at room T and c) platinum nanoparticles formed on the surface of the zeolite and d) dispersed platinum nanoclusters obtained after reduction of the $PtCl_6^{2-}$/MOR and $Pt(NH_3)_4^{2+}$/MOR samples, at 110 °C.**

On the other hand, when the sample was impregnated with $Pt(NH_3)_4^{2+}$ and was reduced with formic acid, agglomerated platinum nanoclusters were formed inside zeolite mordenite. The average diameter of the nanoclusters was 5 nm (StDev = 2 nm). The agglomeration of the platinum nanoclusters suggests a poor distribution of the reducing agent into the zeolite at room temperature.

When the same reduction method was done at 110 ° C, however, nanoparticles with an average diameter of 11 nm (StDev = 5) were formed on the surface of the zeolite when using $PtCl_6^{2-}$ and 3.6 nm well dispersed nanoclusters (StDev = 0.8 nm) are formed inside the zeolite. The fact that more isotropic and smaller nanostructures are formed at this temperature agrees with the fact that at higher temperatures the reduction is diffusion limited, that is, the reaction rate is higher than the diffusion rate leading to smaller nanoparticles. This temperature is also slightly higher than the normal boiling temperature of the formic acid so it is expected that it behaves more like a gas phase reducing agent.

The reduction of a $PtCl_6^{2-}$/MOR sample with ethylene glycol at 110 °C promoted the formation of multipod platinum nanostructures with an average diameter of 24 nm (StDev = 10 nm) as shown in Figure 2.4(a).Similar Pt multipod structures have been obtained in soft templates, however, that in those previous reports extraneous inorganic substances such as $NaNO_3$ and Ag(acac) were necessary to form the multipodic structures. [23, 24, 26] This suggests that here the zeolite has an active role in affecting the anisotropy of the platinum structures.

The TEM image in Figure 2.4(b) shows the formation of 5 nm nanoclusters (StDev = 1.4 nm) in mordenite, after the reduction of $Pt(NH_3)_4^{2+}$/MOR with ethylene glycol. These results show a better nanoparticle distribution in comparison to the nanoclusters obtained with formic acid at room temperature and a comparable nanoparticle size and distribution at the same temperature (110 °C). This temperature was below the normal boiling point of ethylene glycol, which suggests that the temperature is a factor more influential than the phase of the reducing agent in the formation of nanoclusters when using $Pt(NH_3)_4^{2+}$ in mordenite.

When the same experiment was done at 200°C, 14.5 nm diameter nanoparticles (StDev = 6 nm) were formed on the surface of the zeolite when using $PtCl_6^{2-}$ as a precursor and nanoclusters of 3 nm in diameter (StDev = 1 nm) were formed inside the zeolite when $Pt(NH_3)_4^{2+}$ was used (Figure 2.4 (c) and (d), respectively). This temperature was above the normal boiling temperature of the ethylene glycol and it is evident that the tendency towards the formation of anisotropic nanostructures when using $PtCl_6^{2-}$ is gone and smaller nanoclusters are formed with $Pt(NH_3)_4^{2+}$ at this temperature. This suggests that the temperature and phase change affected the reduction of the $PtCl_6^{2-}$ more dramatically than the $Pt(NH_3)_4^{2+}$.

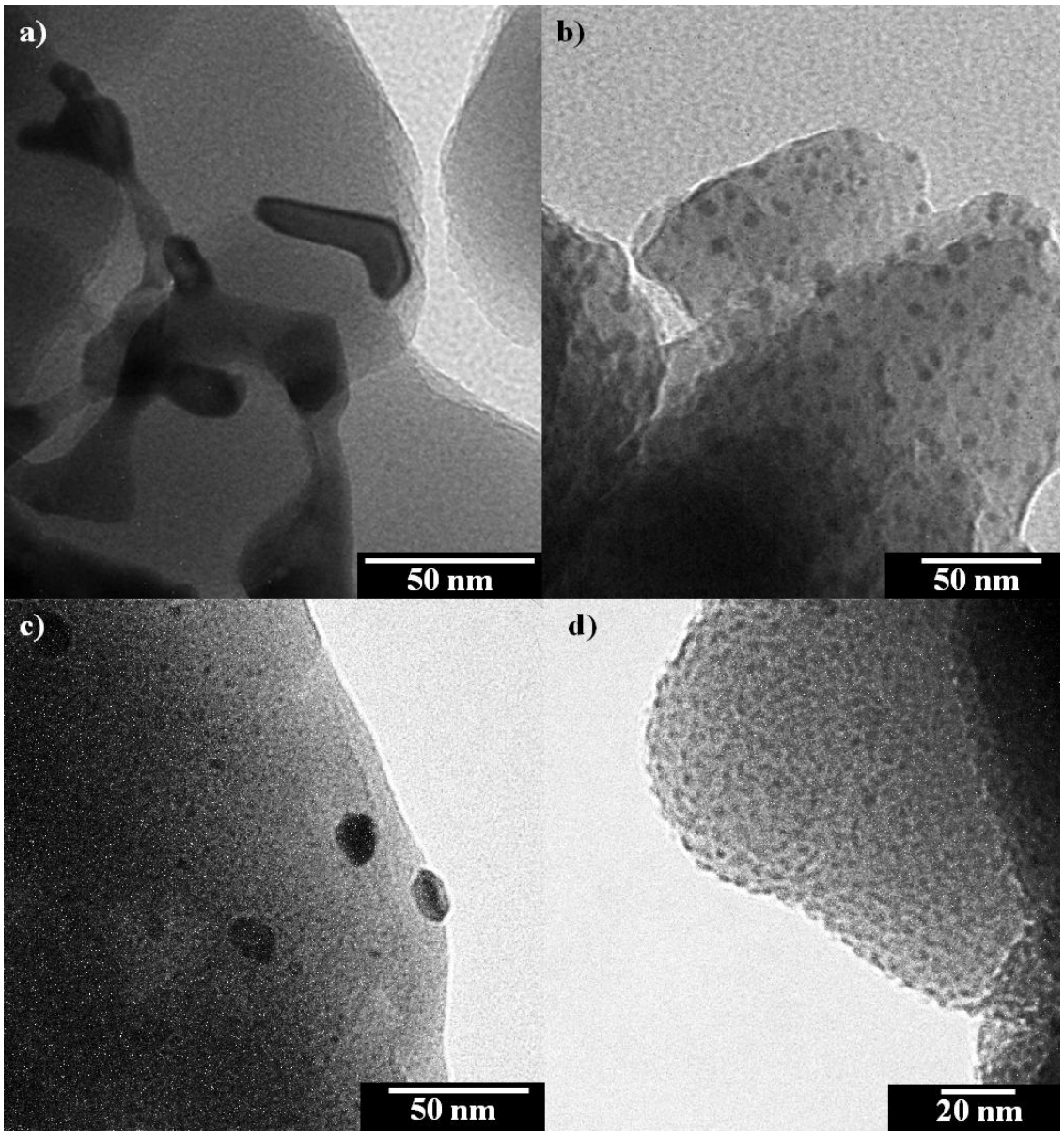

Figure 2.4 **Bright field TEM images of (a) platinum multipod and (b) platinum nanoclusters formed in $PtCl_6^{2-}$/MOR and $Pt(NH_3)_4^{2+}$/MOR, respectively after reduction with ethylene glycol at 110°C, (c) and (d) platinum nanoclusters obtained after reduction of the $PtCl_6^{2-}$/MOR and $Pt(NH_3)_4^{2+}$/MOR samples with ethylene glycol at 200 °C.**

Figure 2.5 shows the Pt nanoclusters formed for the samples reduced with method E on the surface of the sample reduced with UV. In the $PtCl_6^{2-}$/MOR sample (Figure 2.5(a)) the Pt clusters were located on the surface of the zeolite with an average size of 5.3 nm (StDev = 1.2 nm) while in the $Pt(NH_3)_4^{2+}$/MOR sample (Figure 2.5(b)) they were well dispersed inside the zeolite pores with an average size of 1.5 nm (StDev = 0.5 nm). Even though the UV took 48 hours to reduce the platinum precursor, this method yielded the most dispersed nanoparticles found of any of the reduction methods reported here. In fact, these results are comparable to results obtained through very strict traditional catalyst synthesis conditions. This is probably due to the fact that there was no driving force for the diffusion of the Pt atoms as there was no reducing agent flowing through the pores of the zeolite. It is also possible that the methanol is acting as a capping agent much like the water in the water-saturated hydrogen reduction method.

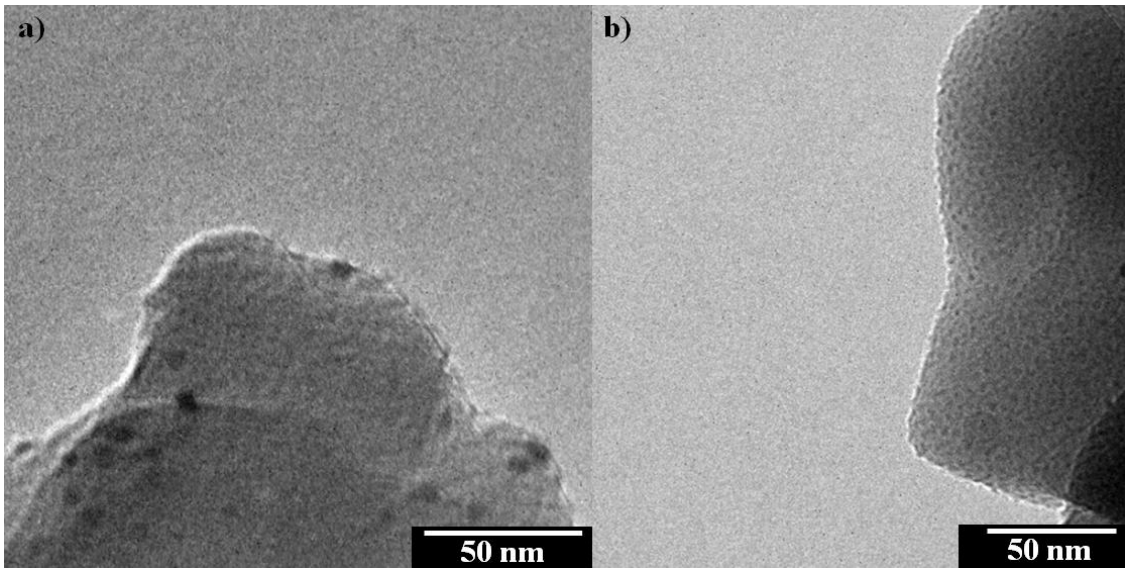

Figure 2.5 Bright field TEM images of nanoclusters formed in (a) sample $PtCl_6^{2-}$/MOR and (b) $Pt(NH_3)_4^{2+}$/MOR synthesized by UV-photoreduction

Finally, the TEM images of the samples reduced with reduction method F are shown in Figure 2.6. Figure 2.6(a) corresponds to the $PtCl_6^{2-}$/MOR sample and it shows the formation of large and small nanoparticles with irregular shapes formed on the surface of the zeolite. On the other hand, platinum nanowires with diameters in the range of 8 - 60 nm were formed inside of the zeolite mordenite when $Pt(NH_3)_4^{2+}$ was used as precursor as shown in Figure 2.6(b). The nanowires are evident as dark stripes around the external surface area of the zeolite. These results demonstrate that KBH_4 is efficient for the formation of nanowires in porous materials when used in the solid state. This method is explored further in Chapters 3 and 4.

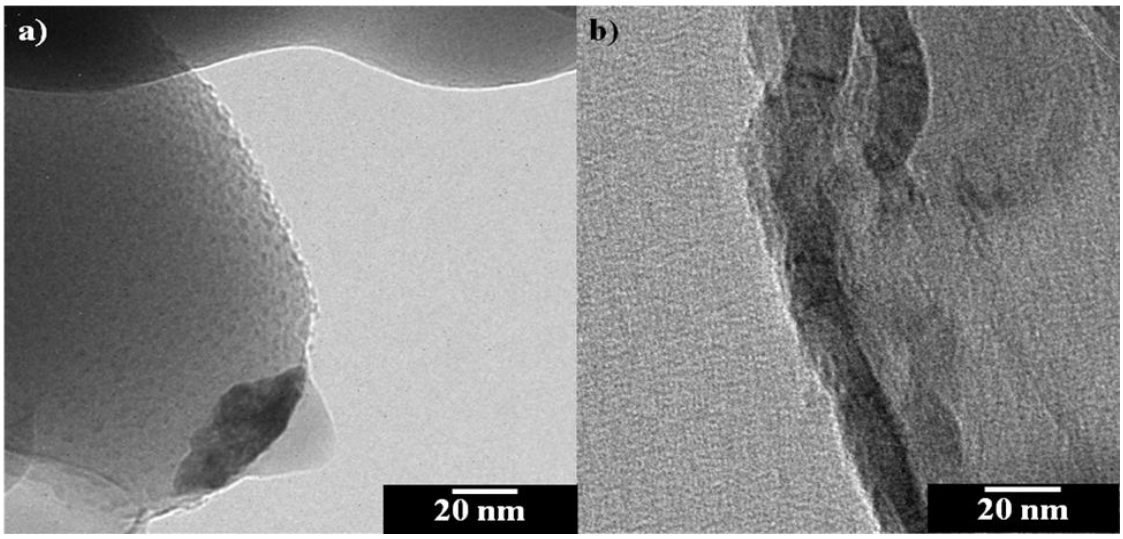

Figure 2.6 Bright field TEM images of (a) platinum nanoclusters and (b) platinum nanowires formed in $PtCl_6^{2-}$/MOR and $Pt(NH_3)_4^{2+}$/MOR, respectively after solid state reduction with KBH_4.

The formation of platinum nanowires using this method could be explained as an anodic electrochemical reaction that starts in the external surface of the zeolite. The slow evolution of this reaction promotes the migration and diffusion of positive platinum precursors from the internal zone of the zeolite towards the surface. Progressively, the positive platinum precursors that reach the platinum surface are reduced by the transfer of electrons promoting the formation of nanowires. In this process the KBH_4 is thought to have a very poor penetration into the pores of the zeolite such that it stays mainly on the surface.

2.6 Conclusions

There was an evident difficulty of the negatively-charged precursor to diffuse inside the pores of the zeolite. The difficulty is associated with an electrostatic repulsion between the anodic precursor and the negative charges in the pore channels of the zeolite. As a consequence, all the nanostructures formed using this precursor grew unrestricted, forming large clusters on the surface of the zeolite. Nevertheless, there was a characteristic tendency for this precursor to form anisotropic nanostructures on the surface of the clusters as was found in the literature for other systems with the notable effect that the presence of the zeolite promoted the formation of a bigger core. Perhaps a way to form nanowires in zeolites with this precursor requires a modification of the zeolite's pore charge.

Comparing the results using the reducing agents at different states, it was evident that the anisotropy of the platinum nanostructures formed increased following the sequence of Gas<Liquid<Solid. This can be explained by the hindering of the diffusion of the reducing agent when going to denser phases. Within the same phase it was observed that an anisotropic crystal growth was favorable when the reduction rate was slowed down in comparison to the diffusion of the Pt atoms.

Zeolites have the peculiarity of causing a slow diffusion of molecules due to the size of their pores, causing syntheses to be controlled mostly by the kinetics. Thus, in general, the formation of anisotropic structures inside of the zeolites is difficult when using gas and liquid reducing agents. On the other hand, and as was

observed previously by our group, the use of a solid state reducing agent yielded platinum nanowires inside of the zeolite.

This work shows that the reduction methods studied that have successfully yielded Pt nanowires in other systems, do not achieve similar results when using a zeolite and that a method such as the solid state reduction method is necessary for the formation of such nanostructures in zeolites. It also shows that using reducing agents in the liquid phase on zeolites do not appear to be beneficial for the formation of either dispersed nanoparticles, or nanowires.

Finally, four reduction methods were found that could be further explored to synthesize supported platinum catalysts: through the use of water saturated hydrogen, the use of formic acid and ethylene glycol at temperatures higher than the normal boiling temperature and through UV reduction. In all, the presence of an adsorbed reducing agent (water, formic acid, ethylene glycol, and methanol) could be acting as a capping agent for the growth of the nanoparticles resulting in well dispersed nanoclusters.

References

[1] Xia Y, Yang P (2003) Chemistry and physics of nanowires. Advanced Materials 15:351-352

[2] Hrapovic S, Liu Y, Male KB, Luong JHT (2003) Electrochemical Biosensing Platforms Using Platinum Nanoparticles and Carbon Nanotubes. Analytical Chemistry 76:1083-1088

[3] Chen H, Yuan R, Chai Y, Wang J, Li W (2010) Glucose biosensor based on electrodeposited platinum nanoparticles and three-dimensional porous chitosan membranes. Biotechnology Letters 32:1401-1404

[4] Yang H, Zhu Y (2007) Glucose biosensor based on nano-SiO2 and "unprotected" Pt nanoclusters. Biosensors and Bioelectronics 22:2989-2993

[5] Zhu N, Chang Z, He P, Fang Y (2005) Electrochemical DNA biosensors based on platinum nanoparticles combined carbon nanotubes. Analytica Chimica Acta 545:21-26

[6] Yang M, Yang Y, Liu Y, Shen G, Yu R (2006) Platinum nanoparticles-doped sol-gel/carbon nanotubes composite electrochemical sensors and biosensors. Biosensors and Bioelectronics 21:1125-1131

[7] Yang M, Qu F, Lu Y, He Y, Shen G, Yu R (2006) Platinum nanowire nanoelectrode array for the fabrication of biosensors. Biomaterials 27:5944-5950

[8] Fengli Q, Minghui Y, Guoli S, Ruqin Y (2007) Electrochemical biosensing utilizing synergic action of carbon nanotubes and platinum nanowires prepared by template synthesis. Biosensors and Bioelectronics 22:1749-1755

[9] Sasaki M, Osada M, Sugimoto N, Inagaki S, Fukushima Y, Fukuoka A, Ichikawa M (1998) Novel templating fabrication of nano-structured Pt clusters and wires in the ordered cylindrical mesopores of FSM-16 and their unique properties in catalysis and magnetism. Microporous and Mesoporous Materials 21:597-606

[10] Adhyapak PV, Karandikar P, Vijayamohanan K, Athawale AA, Chandwadkar AJ (2004) Synthesis of silver nanowires inside mesoporous MCM-41 host. Materials Letters 58:1168-1171

[11] Tiemann M (2007) Repeated Templating. Chemistry of Materials 20:961-971

[12] Sakamoto Y, Fukuoka A, Higuchi T, Shimomura N, Inagaki S, Ichikawa M (2003) Synthesis of Platinum Nanowires in Organica Inorganic Mesoporous Silica Templates by Photoreduction: Formation Mechanism and Isolation. Journal of Physical Chemistry B 108:853-858

[13] Chen A, Holt-Hindle P (2010) Platinum-Based Nanostructured Materials: Synthesis, Properties, and Applications. Chemical Reviews 110:3767-3804

[14] Song Y, Garcia RM, Dorin RM, Wang H, Qiu Y, Coker EN, Steen WA, Miller JE, Shelnut JA (2007) Synthesis of platinum nanowire networks using a soft template. Nano Letters 7:3650-3655

[15] Webb P, Orr C, Camp R, Olivier J, Yunes Y (1997) Analytical Methods in Fine Particle Technology. Micromeritics Instrument Corporation, USA

[16] Napolskii KS, Barczuk PJ, Vassiliev SY, Veresov AG, Tsirlina GA, Kulesza PJ (2007) Templating of electrodeposited platinum group metals as a tool to control catalytic activity. Electrochimica Acta 52:7910-7919

[17] Araki H, Fukuoka A, Sakamoto Y, Inagaki S, Sugimoto N, Fukushima Y, Ichikawa M (2003) Template synthesis and characterization of gold nano-wires and -particles in mesoporous channels of FSM-16. Journal of Molecular Catalysis A: Chemical 199:95-102

[18] Fukuoka A, Sakamoto Y, Higuchi T, Shimomura N, Ichikawa M (2006) Synthesis and electronic property of platinum nanowire and nanoparticle in mesoporous silica template. Journal of Porous Materials 13:231-235

[19] Fukuoka A, Higashimoto N, Sakamoto Y, Inagaki S, Fukushima Y, Ichikawa M (2002) Preparation, XAFS Characterization, and Catalysis of Platinum Nanowires and Nanoparticles in Mesoporous Silica FSM-16. Topics in Catalysis 18:73-78

[20] Fukuoka A, Higuchi T, Ohtake T, Oshio T, Kimura J-i, Sakamoto Y, Shimomura N, Inagaki S, Ichikawa M (2006) Nanonecklaces of Platinum and Gold with High Aspect Ratios Synthesized in Mesoporous Organosilica Templates by Wet Hydrogen Reduction. Chemistry of Materials 18:337-343

[21] Fukuoka A, Higashimoto N, Sakamoto Y, Sasaki M, Sugimoto N, Inagaki S, Fukushima Y, Ichikawa M (2001) Ship-in-bottle synthesis and catalytic performances

of platinum carbonyl clusters, nanowires, and nanoparticles in micro- and mesoporous materials. Catalysis Today 66:23-31

[22] Yang C-M, Sheu H-S, Chao K-J (2002) Templated Synthesis and Structural Study of Densely Packed Metal Nanostructures in MCM-41 and MCM-48. Advanced Functional Materials 12:143-148

[23] Chen J, Herricks T, Geissler M, Xia Y (2004) Single-Crystal Nanowires of Platinum Can Be Synthesized by Controlling the Reaction Rate of a Polyol Process. Journal of the American Chemical Society 126:10854-10855

[24] Herricks T, Chen J, Xia Y (2004) Polyol Synthesis of Platinum Nanoparticles: Control of Morphology with Sodium Nitrate. Nano Letters 4:2367-2371

[25] Sun S, Yang D, Villers D, Zhang G, Sacher E, Dodelet J (2008) Template- and Surfactant-free Room Temperature Synthesis of Self-Assembled 3D Pt Nanoflowers from Single-Crystal Nanowires. Advanced Materials 20:571-574

[26] Teng X, Yang H (2005) Synthesis of Platinum Multipods: An Induced Anisotropic Growth. Nano Letters 5:885-891

[27] Chakarova K, Hadjiivanov K, Atanasova G, Tenchev K (2007) Effect of preparation technique on the properties of platinum in NaY zeolite: A study by FTIR spectroscopy of adsorbed CO. Journal of Molecular Catalysis A: Chemical 264:270-279

[28] Yang Y-X, Bourgeois L, Zhao C, Zhao D, Chaffee A, Webley PA (2009) Ordered micro-porous carbon molecular sieves containing well-dispersed platinum

nanoparticles for hydrogen storage. Microporous and Mesoporous Materials 119:39-46

[29] Quiñones L, Grazul J, Martínez-Iñesta MM (2009) Synthesis of platinum nanostructures in zeolite mordenite using a solid-state reduction method. Materials Letters 63:2684-2686

[30] Sakamoto Y, Fukuoka A, Higuchi T, Shimomura N, Inagaki S, Ichikawa M (2003) Synthesis of Platinum Nanowires in Organica Inorganic Mesoporous Silica Templates by Photoreduction: Formation Mechanism and Isolation. The Journal of Physical Chemistry B 108:853-858

[31] Kubanek P, Schmidt HW, Spliethoff B, Schüth F (2005) Parallel IR spectroscopic characterization of CO chemisorption on Pt loaded zeolites. Microporous and Mesoporous Materials 77:89-96

[32] Ismagilov ZR, Yashnik SA, Startsev AN, Boronin AI, Stadnichenko AI, Kriventsov VV, Kasztelan S, Guillaume D, Makkee M, Moulijn JA (2009) Deep desulphurization of diesel fuels on bifunctional monolithic nanostructured Pt-zeolite catalysts. Catalysis Today 144:235-250

[33] Rivallan M, Seguin E, Thomas S, Lepage M, Takagi N, Hirata H, Thibault-Starzyk F (2010) Platinum Sintering on H-ZSM-5 Followed by Chemometrics of CO Adsorption and 2D Pressure-Jump IR Spectroscopy of Adsorbed Species. Angewandte Chemie International Edition 49:785-789

[34] Rees L, Shen D (2001) In: Jansen J (ed) Studies in surface science and catalysis 137. Elsevier science, Amsterdam

Chapter 3 SYNTHESIS OF PLATINUM NANOSTRUCTURES IN ZEOLITE MORDENITE USING SOLID-STATE REDUCTION

Abstract

Platinum nanoparticles and nanowires have been synthesized inside zeolite mordenite using solid state reduction. Tetramine platinum nitrate was introduced into the pores via incipient wetness impregnation and it was reduced using powder sodium borohydride. With this method it was possible to obtain single crystal nanowires along the edges of the zeolite particle while using a regular aqueous sodium borohydride solution reduction no nanowires were obtained. The molar ratio of the reducing agent to platinum atoms was a critical parameter for the formation of either uniform nanoparticles or nanowires.

3.1 Introduction

The potential uses of nanowires are varied [1] and include areas such as drug delivery [2, 3], cancer treatment [4, 5],biosensors [6], reaction catalysis [7], and magnetic data storage [8]. Specifically, integrated sensor devices based on platinum nanowires have been reported to provide higher sensitivity, improved signal-to-noise ratio (S/N), and a diminution of the threshold detection limit [9]. Furthermore, platinum nanowires could play an important role as either interconnection elements or as active components in nanoscale electronic devices [1, 10].

As already described in Chapter 2, the synthesis of metal nanowires has been reported using various solid-state porous templates such as mesoporous silica, MCM-41, MCM-48 [11], SBA-15 [12], FSM-16 [13], HMM-1 [14], and the organosilica HMM [15].

Another reduction method that has been widely studied for the synthesis of metal nanostructures is the chemical reduction by an aqueous $NaBH_4$ solution. In MCM-41, for example, 2.8 nm silver nanowires were formed by a dropwise addition of $NaBH_4$ solution to an aqueous solution of suspended MCM-41 and $AgNO_3$ [16]. This method has also been reported to form small Pt nanowires using other types of templates [17, 18].

This chapter presents experimental method for the synthesis of nanostructures using zeolite mordenite. Single crystal Pt nanowires and very monodisperse nanoparticles were obtained depending on the synthesis conditions.

3.2 Experimental Section

Zeolite mordenite with Si/Al = 6.5 was obtained from Zeolyst International (CBV-10A). Five samples are reported here: samples A, B, C and D that were treated under different conditions. The zeolite used for all samples underwent a rigorous pretreatment to remove any impurity in the pore of the zeolite in vacuum at 400°C.

The metal loading for all the samples was 5% wt Pt which was incorporated using incipient wetness impregnation. A typical procedure consisted of making an aqueous solution made up of 26.1 mg of tetra-amine platinum (II) nitrate [$Pt(NH_3)_4(NO_3)_2$ - Aldrich, USA] in 210 µl of deionized water. This solution was added drop by drop to 250 mg of the zeolite until saturation. The Pt loaded zeolite was dried at room temperature for 30 min to remove the water excess.

For the reduction two main approaches were followed using $NaBH_4$. For the samples (A, B, and C) the solid-state reduction method was used. In this procedure the Pt impregnated zeolite powder was thoroughly mixed with sodium borohydride powder ($NaBH_4$ 98% - Alfa Aesar) using a spatula to contact the reducing agent and the impregnated zeolite. Samples A was reduced using 25 mg of $NaBH_4$ ($NaBH_4$/Pt = 9.8); sample B was reduced using 9 mg of $NaBH_4$ ($NaBH_4$/Pt =3.55) and sample C was reduced using 2.53 mg of $NaBH_4$ ($NaBH_4$/Pt =1/1).

As a reference sample D was reduced following the method reported by Adhyapak et al. [16]. Here 250 mg of pretreated mordenite was put into contact with a

solution of 0.026 g of $Pt(NH_3)_4(NO_3)_2$ in 100 mL of deionized water. After this solution was stirred for 2h, a solution of 25 mg of $NaBH_4$ in 1 mL of water was added drop by drop. This second solution was left stirring for 24 h after which it was filtered with deionized water.

TEM analyses were performed on a FEI Tecnai T12 and Carl Zeiss Leo 992. EDAX was acquired with a Genesis X-ray detector in a FEI Tecnai T12. HRTEM images were recorded on a FEI Tecnai T20. X-ray diffraction pattern (XRD) were acquired using a RigakuUltima III (λ=0.154 nm, Cu Kα, 40 kV 44 mA). FTIR spectrums of the sample were acquired using a Varian 800 FT-IR spectrometer with ZnSe ATR holder.

3.3 Results and Discussion

The X-ray diffraction pattern of sample A is shown in Figure 3.1. This Figure shows that the solid state reduction method did not modify or damage the original structure of the zeolite framework, as the peaks of the mordenite structure (MOR) are still present in the XRD. The diffraction pattern of sample A shows a peak at $2\theta = 39.8°$ characteristic of the Pt <111> plane that evidences the formation of a Pt fcc crystalline structure. Figure 3.1 also shows that the baseline of the diffraction pattern of sample A has an upward trend with respect to mordenite (MOR) as the diffraction angles increase. This result may be an indication of a loss of crystallinity of the mordenite due to a possible rupture of pores by the growth of the nanowires.

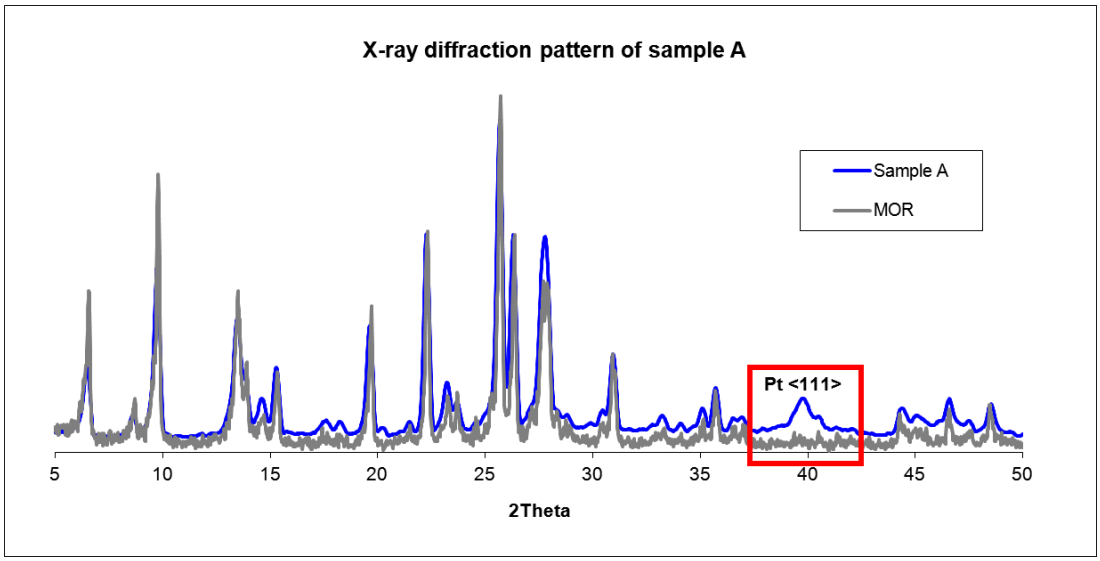

Figure 3.1 XRD patterns of zeolite mordenite (MOR) and Pt Nanowires/mordenite (Sample A).

Figure 3.2 shows the corresponding bright field TEM images of sample A. It shows that through the solid state reduction method fairly uniform nanowires with an apparent diameter of 6.57 nm were formed mainly along the perimeter of the zeolite.

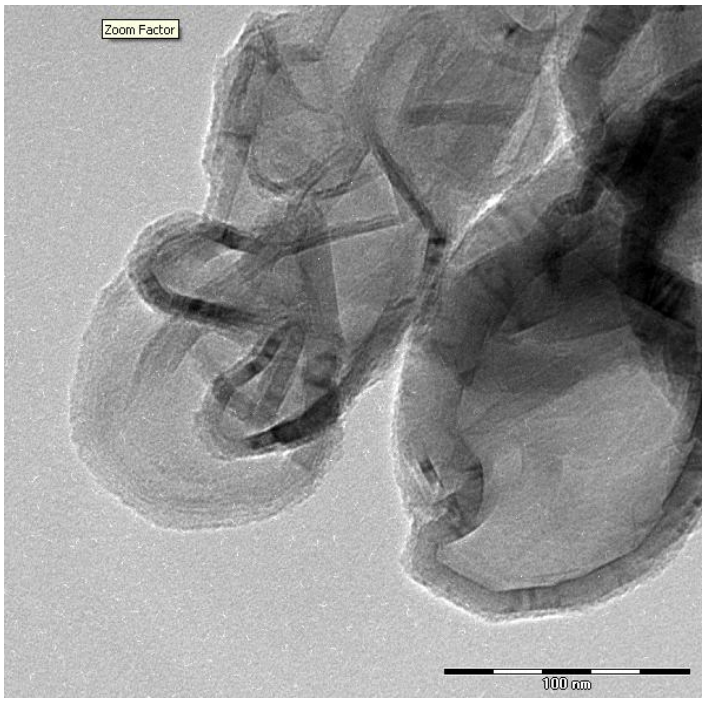

Figure 3.2 Bright Field TEM image of the platinum nanowires formed along the perimeter of a mordenite particle in Sample A reduced with a $NaBH_4$: Pt = 10

The fact that the nanowires form along the surface of the zeolite suggests that the formation of the nanowires depends strongly on the contact area between the reducing agent and the impregnated zeolite particle.

The chemical composition of this sample was analyzed by energy dispersion analysis of X-ray (EDAX) and the results are shown in Figure 3.3. The spectrum shows the presence of the oxygen, aluminum and silicon atoms of the zeolite, in addition to the platinum atoms that make up the nanowires, showing that the nanowires were in fact Pt. It also shows that there are no remaining impurities from

the synthesis in the sample suggesting that all the byproducts of the reduction reaction do not remain on the sample. The unidentified peak in Figure 3.3 corresponds to element Cu from the TEM cooper grid.

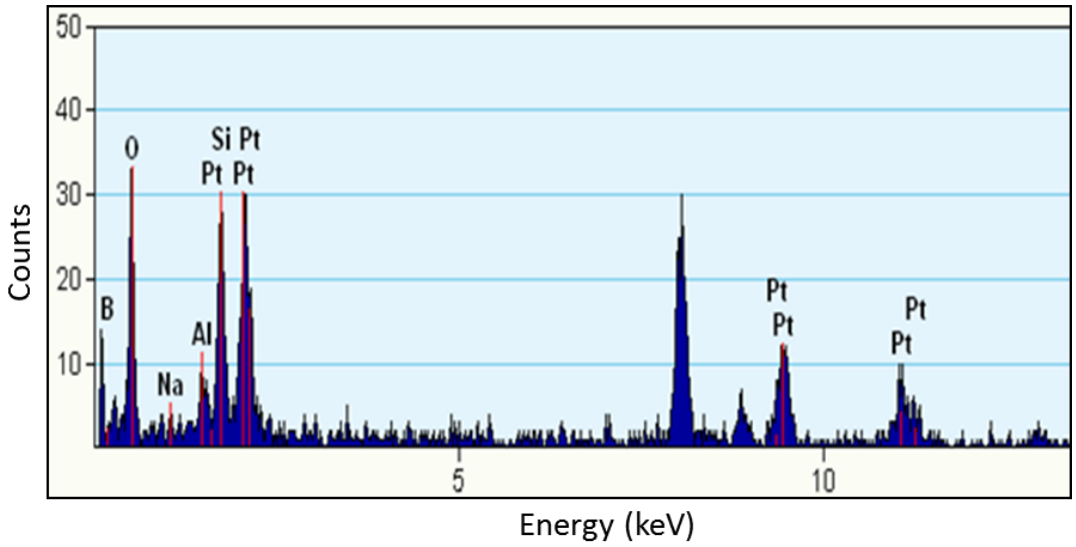

Figure 3.3 EDAX spectrum acquired from sample A.

High resolution scanning transmission electron microscopy (HRSTEM) images were obtained from this sample to look at the characteristics of the nanowires as shown in Figure 3.4. Figure 3.4(a) shows a HRSTEM image in the bright field mode. Here, the background of the micrograph is bright and the dark stripes correspond to the imaging of the platinum nanowires. Figure 3.4(b) shows a dark field TEM image of the same area. In this mode, a diffracted beam is obtained through a HAADF detector, and due to the high scattering of the platinum atoms they appear

bright, while the Si, O and Al atoms from the zeolite appear darker. In this image it is possible to clearly observe the directionality of the Pt planes in the nanowires.

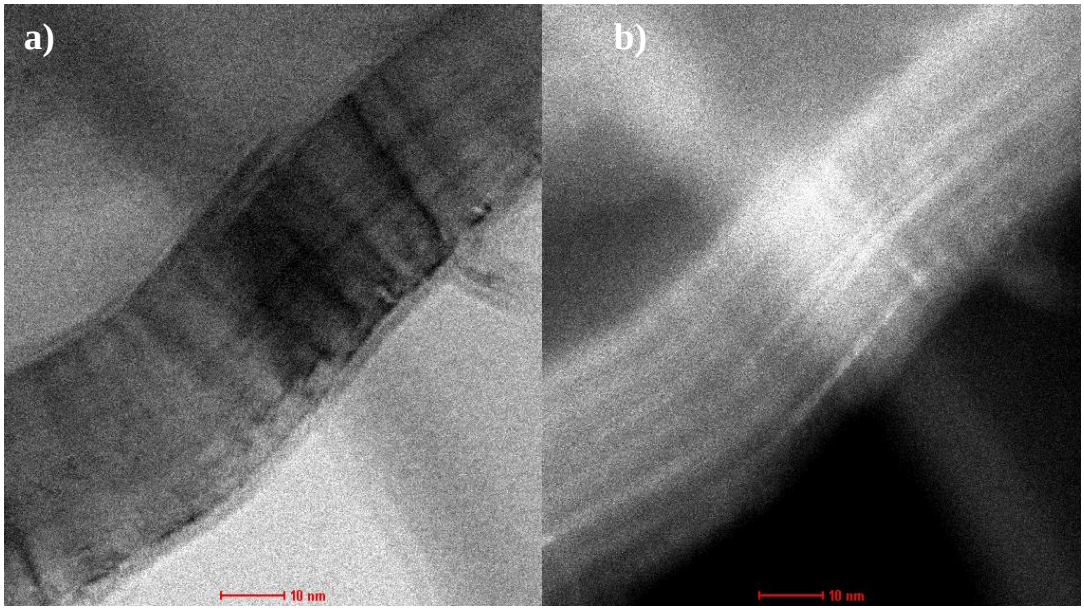

Figure 3.4 TEM images in a) Bright field and b) Dark field of sample A.

A closer look at this sample using HRTEM shows that these nanowires are highly ordered and that they grow along the Pt <100> direction which is quite unusual for these nanowires (see Figure 3.5).

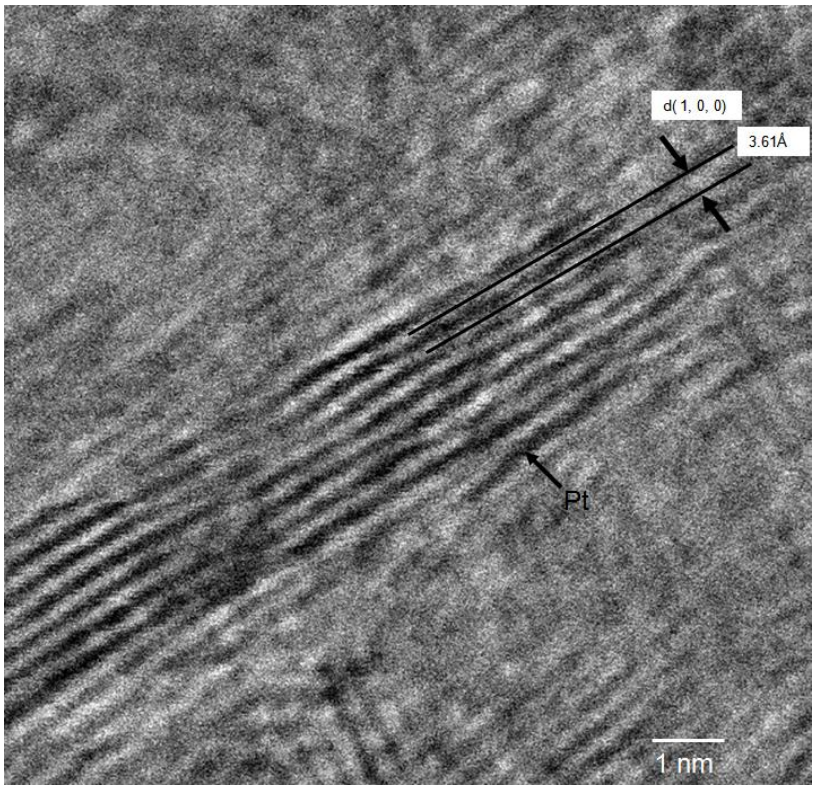

Figure 3.5 Bright field HRTEM image of platinum nanowires in mordenite for sample A which shows the highly ordered nature of the nanowires.

The fact that this solid-state reduction method was successful in the formation of nanowires has many implications. The first and most important is that the friction between the solid $NaBH_4$ and the impregnated zeolite and ambient water were enough to unlock the reducing power of sodium borohydride. $NaBH_4$ is a strong reducing agent but, as evidenced in published works, its reducing properties have been mainly studied in bulk aqueous solutions. The fact that $NaBH_4$ can also be used as a reducing agent in the solid state opens up a new range of possible applications for it.

Although the role of ambient water during reduction has not been fully studied, the fact that such a low amount is sufficient to trigger the reduction properties of $NaBH_4$ is a step forward towards the localized growth of nanostructures.

To test these ideas samples B and C were studied using different $NaBH_4$/Pt molar ratios. Sample B resulted in the formation of platinum nanoparticles while for sample C no nanoparticle formation was apparent. The Pt nanoparticles obtained for sample B (Figure 3.6) had an average 1.8 nm diameter and it was apparent that nanoparticles were present not only on the surface of the zeolite. This corroborates the reduction properties of the powder $NaBH_4$ but it also evidences that the contact area between the two is critical for the formation of elongated nanostructures instead of nanoclusters. The fact that very monodisperse nanoparticles are formed with this method suggests that this will be very useful to fields such as catalysis.

Finally the bright field TEM image of sample D (Figure 3.7) shows that reduction using an aqueous $NaBH_4$ solution in zeolite mordenite yields nanoclusters instead of nanowires. For this sample nanoparticles with an average 2.77 ± nm diameter were formed mainly on the outside surface of the zeolite. This suggests that in zeolites, as opposed to mesoporous silicas studied by Adhyapak et al. [16], the amount of water needs to be controlled in order to obtain nanowires and that a solid state reduction process such as the one presented here is in fact needed.

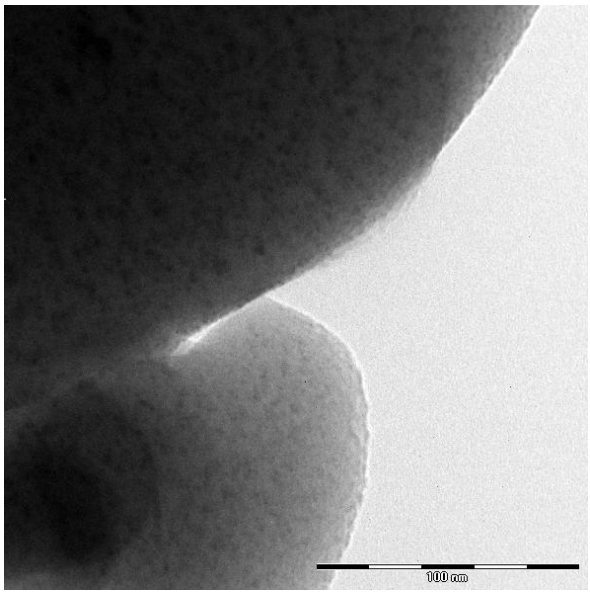

Figure 3.6 Bright field TEM image of the platinum nanoparticles formed inside mordenite in sample B reduced with a $NaBH_4$: Pt = 3.55

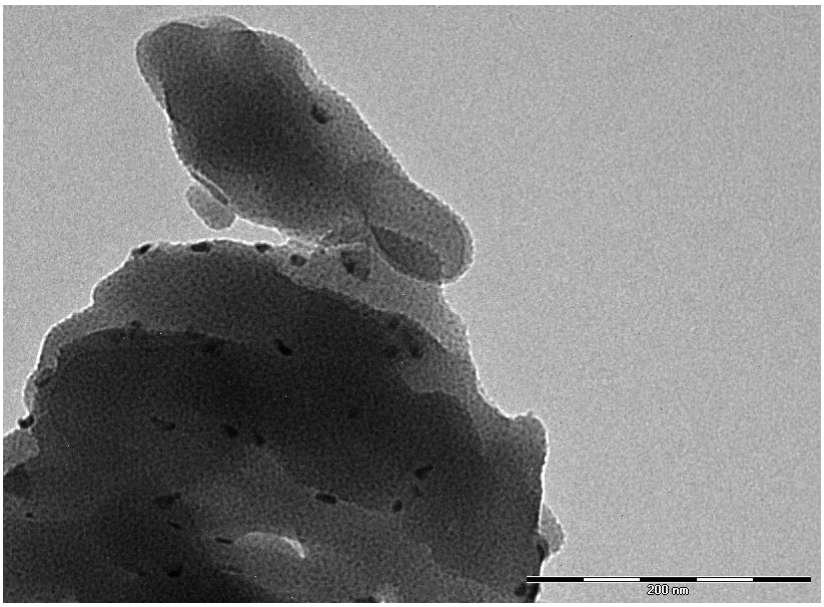

Figure 3.7 Bright Field TEM image of the platinum nanowires formed on the surface of mordenite in sample D reduced using an aqueous solution of $NaBH_4$.

Due to the obvious influence the water has on the formation of the platinum nanowires, the effect of the waiting period between impregnation and reduction was also studied. Figure 3.8 shows the TEM image of a sample reduced immediately after the impregnation. The image clearly shows the formation of nanoclusters on the zeolite surface. This effect is attributed to the fact that the platinum precursors did not have enough time to be incorporated in the zeolite and highlights the importance of the control of the water content during the reduction with this method.

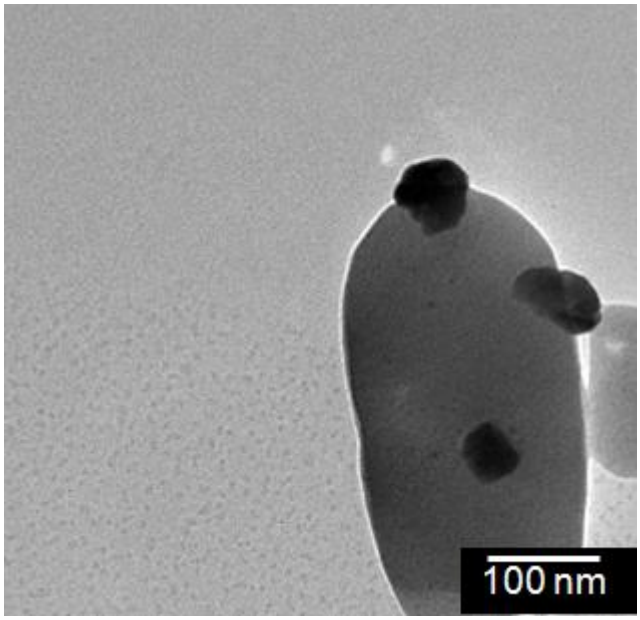

Figure 3.8 Platinum nanoclusters formed in the sample $Pt(NH_3)_4^{2+}$/MOR using solid state reduction method immediately after the impregnation.

Fourier Transform Infrared spectroscopy was used to study the evolution of the reaction in the solid state reduction method. Figure 3.9 shows the results. FTIR

spectrum a) corresponds to zeolite mordenite, spectrum b) was taken from a mordenite sample impregnated with a solution of Tetramineplatinum at a concentration of 5% wt Pt, spectrum c) corresponds to the FTIR sample B that was reduced with a molar ratio of 3.55 of NaBH4 to platinum, and FTIR spectrum d) belongs to sample A, reduced with a molar ratio of NaBH4 to platimum of 9.8.

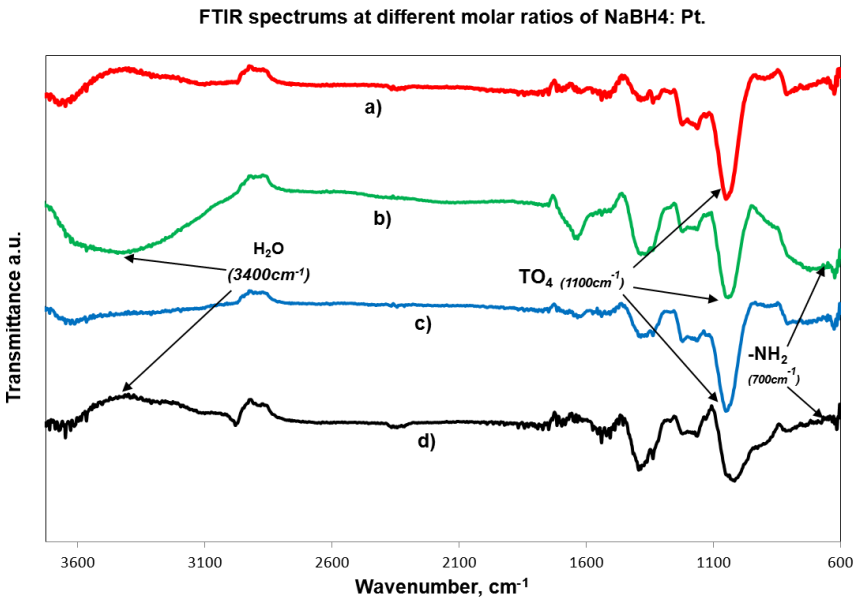

Figure 3.9 FTIR spectrums of a) mordenite, b) mordenite impregnated with a solution of Tetramine platinum (5% wt Pt/mordenite), c) sample B and d) sample A.

FTIR spectrum b) shows the vibrational bands of the functional groups of tetramine platinum, water and mordenite. Vibrational bands at 700 cm^{-1} are attributed

to the NH_2 wagging mode of the Tetramine platinum. Bands observed close to 3400 cm^{-1} are attributed to the presence of water in the sample a), and bands close to 1100 cm^{-1} correspond to the asymmetric stretching vibration of TO_4 from the mordenite (SiO_4 or AlO_4).

The diminishment of the intensity of the vibrational bands at 3400 cm^{-1} and 700 cm^{-1} indicate that the water and amine molecules were detached or consumed from the samples with the decomposition of tetramine platinum. This agrees with EDAX results that during reduction the platinum ligands leave the sample.

3.4 Conclusions

In conclusion, XRD analysis shows that the solid state reduction method does not affect the frame of the zeolite. It is evident that for the successful formation of nanowires in zeolites it is critical that the water used is controlled, such as in the solid state reduction method with waiting time between impregnation and reduction presented here. The relative amount of $NaBH_4$ to zeolite used was also found to be critical for the successful synthesis of nanowires. FTIR studies allowed further understanding of the evolution of the platinum precursos during solid state reduction in mordenite.

References

[1] Xia Y, Yang P (2003) Chemistry and physics of nanowires. Advanced Materials 15:351-352

[2] Panyam J, Labhasetwar V (2004) Sustained Cytoplasmic Delivery of Drugs with Intracellular Receptors Using Biodegradable Nanoparticles. Molecular Pharmaceutics 1:77-84

[3] Collins L, Kaszuba M, Fabre JW (2004) Imaging in solution of (Lys)16-containing bifunctional synthetic peptide/DNA nanoparticles for gene delivery. Biochimica et Biophysica Acta (BBA) - General Subjects 1672:12-20

[4] Zharov VP, Letfullin RR, Galitovskaya EN (2005) Microbubbles-overlapping mode for laser killing of cancer cells with absorbing nanoparticle clusters. Journal of Physics D: Applied Physics 38:2571-2581

[5] Yong Z, Nathan K, Miqin Z (2002) Surface modification of superparamagnetic magnetite nanoparticles and their intracellular uptake. Biomaterials 23:1553-1561

[6] Hrapovic S, Liu Y, Male KB, Luong JHT (2003) Electrochemical Biosensing Platforms Using Platinum Nanoparticles and Carbon Nanotubes. Analytical Chemistry 76:1083-1088

[7] Scott RWJ, Wilson OM, Crooks RM (2005) Synthesis, Characterization, and Applications of Dendrimer-Encapsulated Nanoparticles. The Journal of Physical Chemistry B 109:692-704

[8] Moser A, Takano K, Margulies DT, Albrecht M, Snobe Y, Ikeda Y, Sun S, Fullerton E (2002) Magnetic recording: advancing into the future. Journal of Physics D: Applied Physics 35:157-167

[9] Yang M, Yang Y, Liu Y, Shen G, Yu R (2006) Platinum nanoparticles-doped sol-gel/carbon nanotubes composite electrochemical sensors and biosensors. Biosensors and Bioelectronics 21:1125-1131

[10] Huczko A (2000) Template-based synthesis of nanomaterials. Applied Physics A: Materials Science and Processing 70:365-376

[11] Yang C-M, Sheu H-S, Chao K-J (2002) Templated Synthesis and Structural Study of Densely Packed Metal Nanostructures in MCM-41 and MCM-48. Advanced Functional Materials 12:143-148

[12] Liu Z, Terasaki O, Ohsuna T, Hiraga K, Shin HJ, Ryoo R, Liu Z (2001) An HREM Study of Channel Structures in Mesoporous Silica SBA-15 and Platinum Wires Produced in the Channels. ChemPhysChem 2:229-231

[13] Fukuoka A, Higashimoto, N., Sakamoto, Y., Inagaki, S., Fukushima, Y., Ichikawa, M. (2002) Preparation, XAFS characterization, and catalysis of platinum nanowires and nanoparticles in mesoporous silica FSM-16. . Topics in Catalysis 18(1-2):73-78

[14] Sakamoto Y, Fukuoka A, Higuichi T (2004) Synthesis of Platinum Nanowires in Organic-Inorganic Mesoporous Silica Templates by Photoreduction: formation mechanism and isolation. American chemical society 108:853-858

[15] Fukuoka A, Higuchi T, Ohtake T, Oshio T, Kimura J-i, Sakamoto Y, Shimomura N, Inagaki S, Ichikawa M (2006) Nanonecklaces of Platinum and Gold with High Aspect Ratios Synthesized in Mesoporous Organosilica Templates by Wet Hydrogen Reduction. Chemistry of Materials 18:337-343

[16] Adhyapak PV, Karandikar P, Vijayamohanan K, Athawale AA, Chandwadkar AJ (2004) Synthesis of silver nanowires inside mesoporous MCM-41 host. Materials Letters 58:1168-1171

[17] Song Y, Garcia RM, Dorin RM, Wang H, Qiu Y, Coker EN, Steen WA, Miller JE, Shelnut JA (2007) Synthesis of platinum nanowire networks using a soft template. Nano Letters 7:3650-3655

[18] Xiaowei Teng, Wei-Qiang Han, Wei Ku, Hücker M (2008) Synthesis of Ultrathin Palladium and Platinum Nanowires and a Study of Their Magnetic Properties. Angewandte Chemie International Edition 47:2055-2058

Chapter 4 EVALUATION OF THE SOLID STATE REDUCTION METHOD FOR THE SYNTHESIS OF PLATINUM NANOSTRUCTURES IN MICROPOROUS MATERIALS

Abstract

This work studies the formation of platinum nanostructures in zeolites ECR-5, mordenite and VPI-5 using the solid state reduction method. The effects of the platinum precursor charge, structure of the zeolite, and platinum concentration on the formation of the platinum nanostructures were evaluated. A suggested synthesis mechanism is given in the end for the synthesis of nanowires in zeolites using the solid state reduction method.

4.1 Introduction

As shown in Chapter 2 of this dissertation, it is evident that modern methods to form nanowires in mesoporous material are not directly extrapolated to microporous material with the purpose of obtaining one dimensional platinum nanostrucutres or platinum nanowires [1-3].

Chapter 3 introduces the solid state reduction as a technique developed by our group that permits the formation of one dimensional platinum nanostructures (1-D) using zeolite mordenite, known as the solid state reduction method [4].

This new technique emerges as an alternative route to form metal nanostructures economically and efficiently, with some control over the size and morphology of the nanostructure [4, 5]. In this chapter the effectiveness of the solid state reduction method was evaluated in the formation of platinum nanostructures in other one dimensional pore zeolites:ECR-5(CAN) and VPI-5(VFI) which are compared to the results with mordenite (MOR). The pore sizes of ECR-5 (CAN), mordenite (MOR), and VPI-5 (VFI) are 0.54 nm, 0.65 nm and 1.2 nm, respectively, as described in Chapter 1. The effects of the waiting time after impregnation, charge of the precursor, and the concentration were also evaluated.

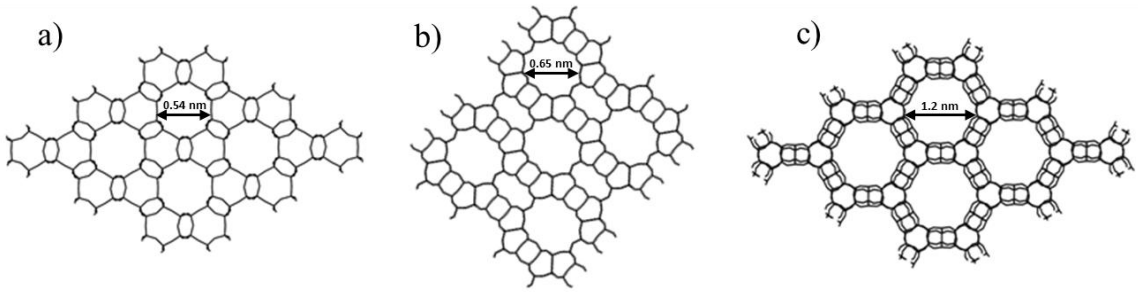

Figure 4.1 Structural frameworks of a) ECR-5 (CAN), b) Mordenite (MOR), and c) VPI-5 (VFI).

4.2 Experimental Section

VPI-5 and ECR-5 zeolites used in these studies were synthesized in the laboratory following the synthesis procedures described in Chapter 1. Mordenite (CVB-10A) with a molar ratio Si/Al of 6.5 was obtained from the company Zeolyst International.

Platinum precursors were incorporated into each of the pretreated zeolites (250 mg) by incipient wetness impregnation (IWI). For the impregnation two aqueous solutions of chloroplatinic acid hydrate ($H_2PtCl_6.H_2O$- Aldrich, USA) and tetramine platinum (II) nitrate ($Pt(NH_3)_4(NO_3)_2$- Aldrich, USA) were prepared by dispersing 27.6 g of chloroplatinic acid hydrate and 26.1 g of tetramine platinum (II) nitrate in 210 µL of distillated/deionized water which were added drop by drop to the sample to achieve a platinum concentration of 5% wt in the samples. Additionally, two samples of zeolite mordenite (250 mg) were loaded with platinum at a concentration of 3% and

1% wt by IWI. The solutions had 15.3 mg and 5 mg of tetramine platinum (II) nitrate [$Pt(NH_3)_4(NO_3)_2$] in 210 µL of distillated/deionized water, respectively. All the impregnated samples were reduced using 25 mg of sodium borohydride and, following the procedure described in previous work from our group [4]. Additionally, a sample of 5% wt Pt/MOR was impregnated with the precursor of tetramine platinum (II) nitrate; the sample was reduced immediately after impregnation to evaluate the effect of time after impregnation on the growth of the platinum nanostructures in the solid state reduction method. Three samples of each were made and studied to verify the reproducibility of the results. The morphology analysis of the platinum nanostructures was done by transmission electron microscopy using a TEM Carl Zeiss Leo 992.

4.3 Results and Discussion

All the zeolite structures were corroborated through X-ray diffraction using a Rigaku Ultima II diffractometer. (See Figure 4.2, 4.3, and 4.4). Platinum nanostructures that were obtained using zeolites ECR-5, mordenite, and VPI-5 impregnated with the chloroplatinic acid precursor are shown in Figure 4.5. Figure 4.5 (a) shows that in $PtCl_6^{2-}$/ECR-5 nanoparticles with an approximate diameter of 39 nm (StDev = 14 nm) were formed on the surface of the zeolite. Figure 4.5 (b) shows that nanoparticles with an average size of 37 nm (StDev = 11) were also formed on the surface of $PtCl_6^{2-}$/MOR and Figure 4.5 (c) shows that nanoparticles with an average size of 25 nm (StDev= 19 nm) were also formed on the surface of the $PtCl_6^{2-}$/VPI-5.

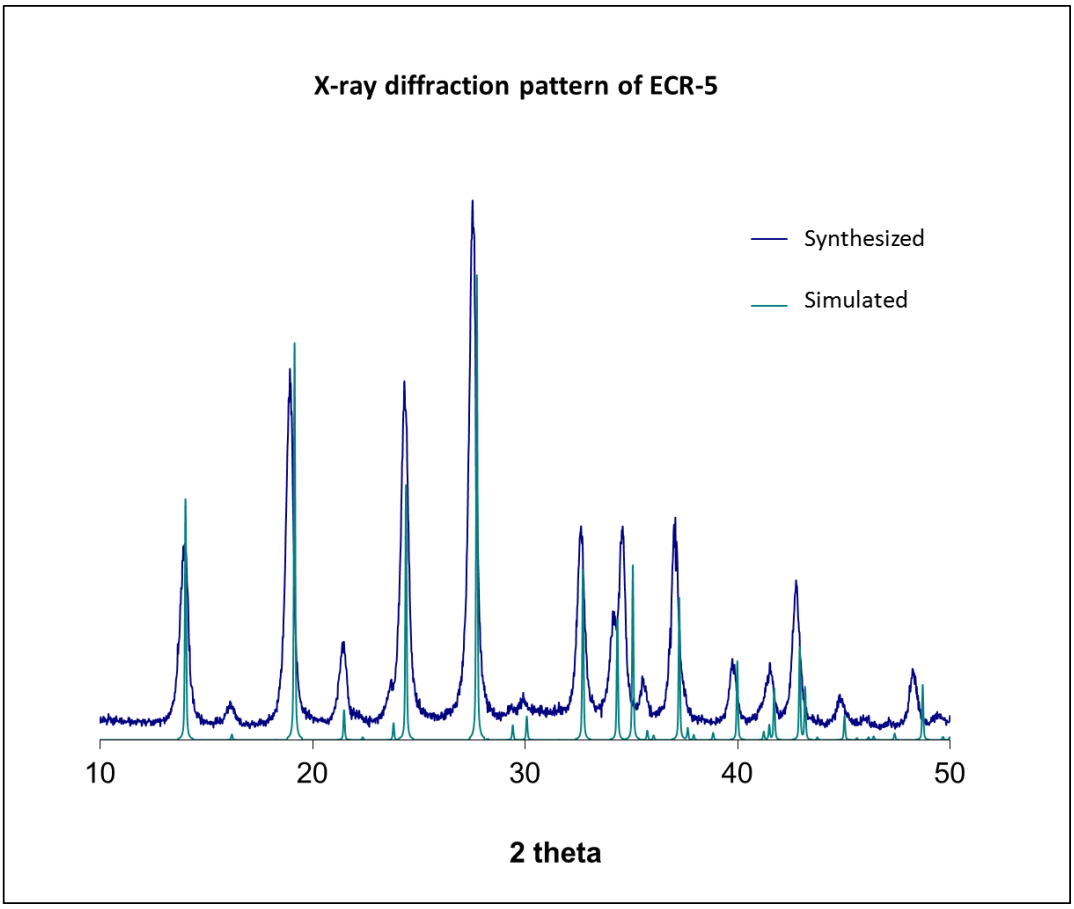

Figure 4.2 **Powder XRD of the as-synthesized ECR-5 compared to the hypothetical XRD.**

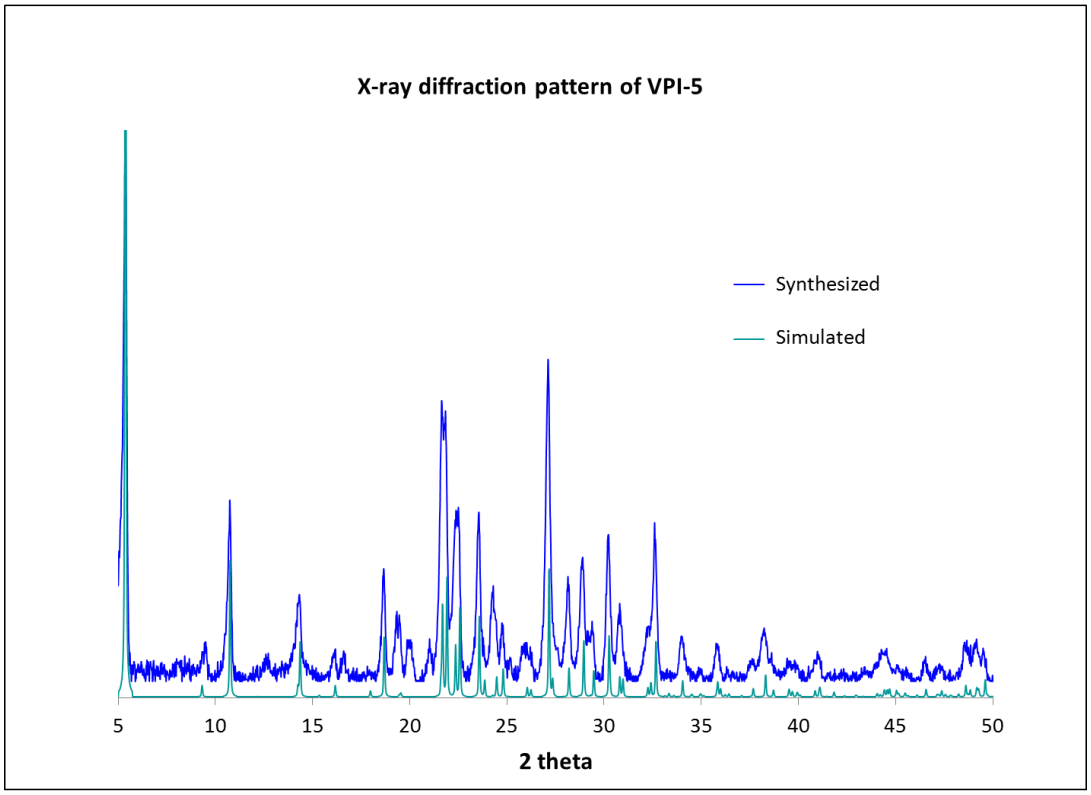

Figure 4.3 **Powder XRD pattern of as-synthesized VPI-5 compared to the hypothetical XRD.**

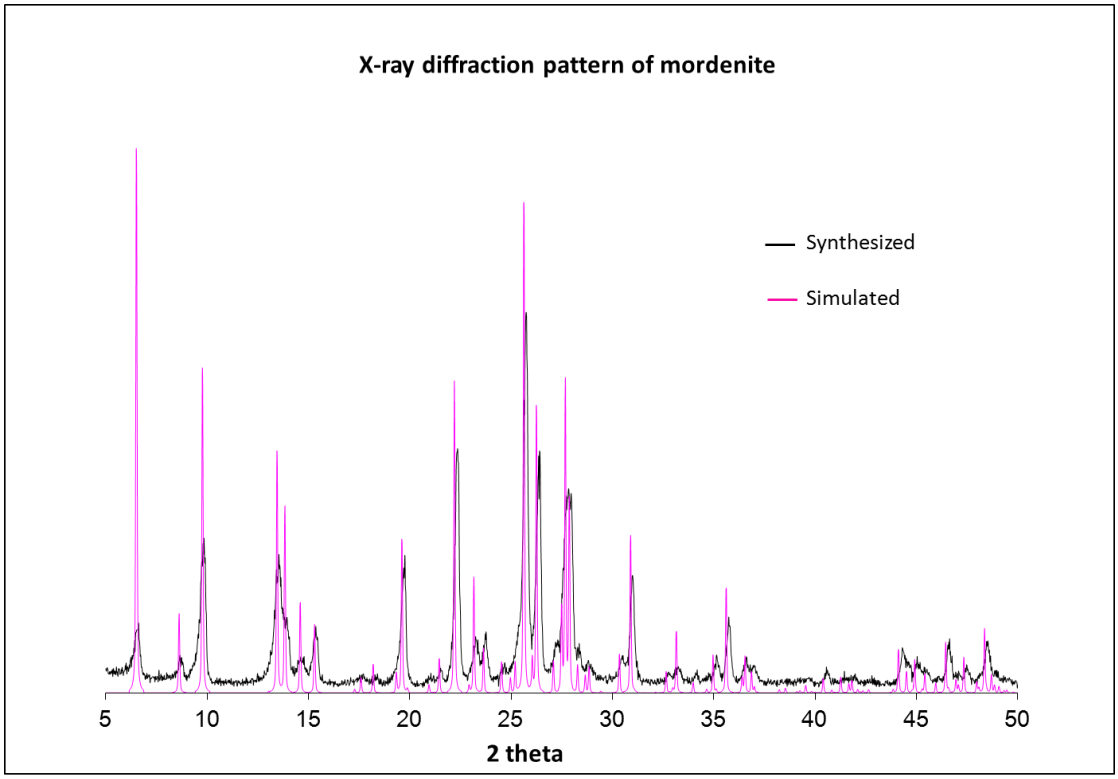

Figure 4.4 Powder XRD of as-received mordenite compared to the hypothetical XRD.

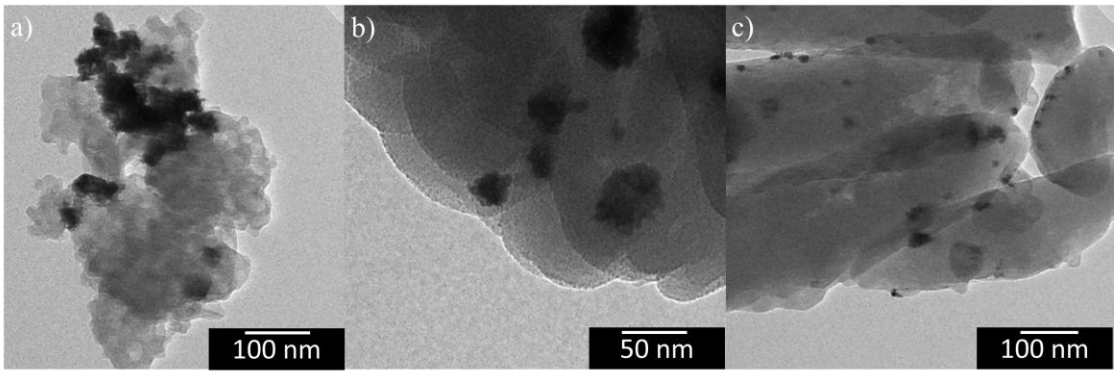

Figure 4.5 TEM images of platinum nanoclusters formed in zeolites (a) VPI-5, (b) ECR-5 and (c) mordenite with a loading of 5%wt Pt using chloroplatinic acid (H_2PtCl_6).

It is evident through these results that chloroplatinic acid had difficulty migrating through the pores of the zeolite. This was something that was observed previously in Chapter 2, but here a direct correlation between the charge of the zeolite and the size of the nanoparticles was also observed.

Zeolites with low Si/Al ratio have larger number of negative charges within of the framework. These charges repel the negative charges of $PtCl_6^{2-}$. This effect combined with the size of the pores, ECR-5 having the smallest, followed by mordenite and then VPI-5 with the largest, contributed to a higher apparent incorporation of the $PtCl_6^{2-}$ into the pores of VPI-5 leading to smaller sizes of platinum nanoparticles. Nevertheless, as was observed before, no nanowires were formed.

TEM images of platinum nanostructures formed in the zeolite samples impregnated with the precursor $Pt(NH_3)_4(NO_3)_2$ are shown in Figure 4.6. The TEM image of the $Pt(NH_3)_4^{2+}$/ECR-5 sample shown in Figure 4.6(a) clearly shows the formation of platinum nanowires with an average diameter of 8 nm (StDev = 4 nm). Figure 4.6(b) shows that in $Pt(NH_3)_4^{2+}$/MOR, platinum nanowires were also formed inside of the zeolite with an approximate diameter of 12 nm (StDev = 6 nm) and Figure 4.6(c) shows that a similar process occurs with $Pt(NH_3)_4^{2+}$/VPI-5, forming nanowires of an average size of 20 nm (StDev = 7 nm). (See Figure 4.6).

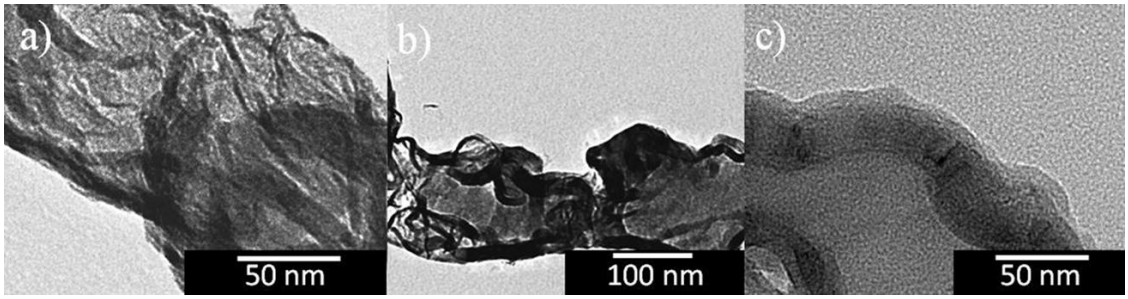

Figure 4.6 TEM image of platinum nanowires inside of the zeolites (a) ECR-5, (b) mordenite and (c) VPI-5 with a loading of 5%wt Pt/zeolite and using $Pt(NH_3)_4(NO_3)_2$ as platinum precursor.

It is clear that the formation of one dimensional nanostructures was facilitated using the positively charged platinum precursor. The fact that the diameter of the nanowires obtained in ECR-5 and MOR are similar and much smaller than those obtained in VPI-5 suggest that, even though the size of the nanowires is one

order of magnitude larger than the size of the zeolites' pores, the pore size does in fact influence the final size of the nanowires. These results also suggest that the $Pt(NH_3)_4^{2+}$ incorporation and the formation mechanism of the nanowires is very similar in the three zeolites studied, despite the fact that VPI-5 is an aluminophosphate with no charge in its structure.

The TEM images shown in Figure 4.7 correspond to the sample loaded with 1%, 3% and 5% wt Pt/MOR. Figure 4.7(a) shows that the platinum nanowires had an approximate diameter of 3.1 nm (StDev = 0.96 nm) when the loading was 1%, while Figure 4.7(b) shows the formation of ~5.78 nm platinum nanowires in the zeolite mordenite with 3% wt Pt. (StDev = 1.27 nm) and Figure 4.7(c) shows that in the sample with a platinum loading of 5% wt the average size of the nanowire was 11.70 nm (StDev = 5.67 nm).

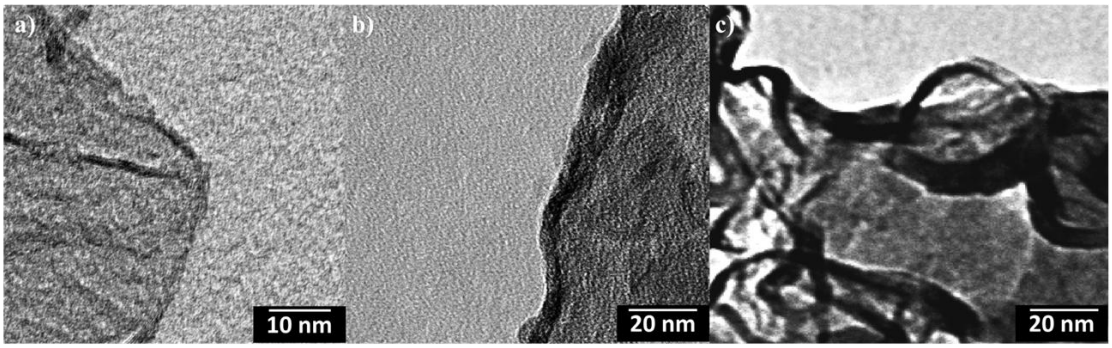

Figure 4.7 TEM image of platinum nanowires in mordenite with a loading of (a) 1%, (b) 3%, (c) 5% wt Pt/zeolite using $Pt(NH_3)_4(NO_3)_2$ as the platinum precursor.

It is evident through the results that there is a direct correlation between the platinum concentration (%wt Pt) and the diameter of the nanowires, which suggests that with this method it is possible to control the size of the nanowires synthesized.

A suggested mechanism for the formation of platinum nanowires that agrees with the results presented in both Chapters 3 and 4 is illustrated in Figure 4.8. Given sufficient time, the tetramine platinum cations diffuse through the channels of the zeolite during impregnation. During the reduction process, the solid state reducing agent is put in contact with the surface of the zeolite. There the borohydride ion spontaneously oxidizes in the presence of water from the zeolite and from the environment, producing a number of electrons according to the reaction 4.1:

$$BH_4^- + 3H_2O \rightarrow BO_3^{3-} + 2H_2 + 6H^+ + 4e^- \qquad \textbf{4.1}$$

The electrons generated on the surface create an electrostatic field that drives the migration of the platinum cations to the surface of the zeolite. When the platinum ions come into contact with the electrons left from the oxidation of the borohydride, they are reduced, forming nanowires in the zeolite's surface. This process is analogous to an electrodeposition synthesis of metal nanowires.

In the case that the negatively charged platinum precursor is used, a repulsion with the negative charge of the zeolite is generated. This makes the incorporation of the platinum in the zeolite difficult and lead the formation of platinum nanoclusters outside of the zeolite.

The use of the zeolites with larger pore sizes appears to improve the diffusion of the platinum precursor to the reduction source, resulting in the formation of platinum nanowires with larger diameters. In the same way a high concentration of platinum in the zeolite leads to a larger amount of platinum atoms to migrate to the reduction area (surface of the zeolite), promoting the formation of platinum nanowires with larger diameters.

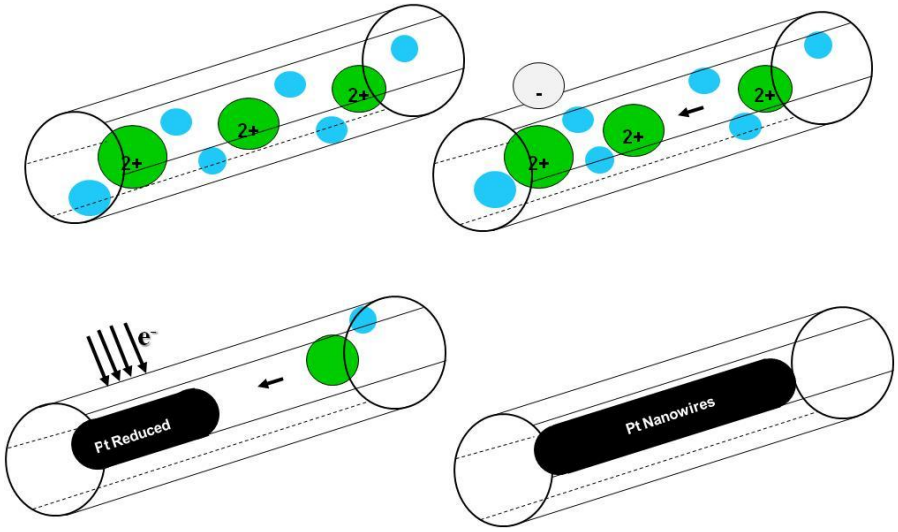

Figure 4.8 Proposed mechanism for the formation of Platinum nanowires inside of the zeolites. (●)=Platinum precursor ($Pt(NH_3)_4^{+2}$), (●) =water (H_2O), (●)=platinum reduced (Pt^0), and (○)=borohydride anion(BH_4^-).

On the other hand, the concentration of the reducing agent also appears to be critical to the formation of a strong enough electrostatic field to induce the diffusion of the platinum precursor to the zeolites' surface to form the nanowires.

Finally, this suggested nanowire formation process also explains why the use of a solid state reduction agent with physical and chemical characteristics similar to sodium borohydride (such as potassium borohydrate) can also be used for the formation of platinum nanowires in zeolites using solid state reduction.

4.4 Conclusions

This Chapter evaluated the growth of platinum nanostructures in zeolites ECR-5, MOR and VPI-5 with solid state reduction method. Platinum nanowires were successfully synthesized in the zeolites. It was found that there is a direct correlation between platinum concentration and nanowire diameter and between zeolite pore size and nanowire diameter.

The results here show that the synthesis of platinum nanowires with the solid state reduction method is applicable to a wide range of zeolitic materials and that it can be fine tuned to control their size. Finally, the formation mechanism proposed suggest that this method could be potentially employed with other porous materials as long as the chosen metal precursor is able to migrate within its pores.

References

[1] Fukuoka A, Higashimoto N, Sakamoto Y, Sasaki M, Sugimoto N, Inagaki S, Fukushima Y, Ichikawa M (2001) Ship-in-bottle synthesis and catalytic performances of platinum carbonyl clusters, nanowires, and nanoparticles in micro- and mesoporous materials. Catalysis Today 66:23-31

[2] Fukuoka A, Higuchi T, Ohtake T, Oshio T, Kimura J-i, Sakamoto Y, Shimomura N, Inagaki S, Ichikawa M (2006) Nanonecklaces of Platinum and Gold with High Aspect Ratios Synthesized in Mesoporous Organosilica Templates by Wet Hydrogen Reduction. Chemistry of Materials 18:337-343

[3] Sakamoto Y, Fukuoka A, Higuchi T, Shimomura N, Inagaki S, Ichikawa M (2003) Synthesis of Platinum Nanowires in Organica Inorganic Mesoporous Silica Templates by Photoreduction: Formation Mechanism and Isolation. Journal of Physical Chemistry B 108:853-858

[4] Quiñones L, Grazul J, Martínez-Iñesta MM (2009) Synthesis of platinum nanostructures in zeolite mordenite using a solid-state reduction method. Materials Letters 63:2684-2686

[5] Kalidindi SB, Sanyal U, Jagirdar BR (2010) Metal Nanoparticles via the Atom-Economy Green Approach. Inorganic Chemistry 49:3965-3967

Chapter 5 MULTIVARIABLE STATISTICAL ANALYSIS

Abstract

In this chapter a multivariable statistical analysis of the cumulative results presented in Chapter 2, followed by the analysis of the formation of Pt nanoparticles using the solid state reduction method for the synthesis of platinum nanostructures in microporous materials presented in Chapters 3 and 4. The end of the chapter presents an overall statistical analysis of all the experimental results in order to understand the main factors that affect the formation of platinum nanostructures in zeolite. The multivariate statistical method used to analyze the experimental results was the Project to Latent Structures Discriminant Analysis (PLS-DA).

5.1 Introduction

Statistical analyses can be classified according to the levels of sophistication. The first level is the OVAT method, the second level is classical statistics and the third and most sophisticated level is the multivariable analysis by projection methods.

5.1.1 One of the variable at time

This is an intuitive method that analyzes each one of the variables at time (OVAT). The OVAT technique is also called the eye-balling method. In this method the average and the standard deviation of each class of observation is computed. After that, the effect of the variables in the analyses is distinguished by testing the difference between the average and standard deviations obtained. The analysis of variables independently makes it difficult to acquire information about of the real correlation between the X and Y variables. For this reason, OVAT is an inefficient method to analyze multivariable data [1].

5.1.2 Classical Methods of Statistics

The second level of sophistication in statistical analyses is what is known as the classical methods of statistics. These methods are: analysis of variance (ANOVA), multiple linear regressions (MLR), design experiment factorial (DOE) and

others. These methods were developed to analyze data with a great number of observations but a small number of evaluated variables.

The underlying assumptions used in these type of methods are the following: The X variables are statistically independent, exact and 100% relevant, the residuals are normally distributed, and the Y variable must be one response, full ranked (continuous) and not qualitative or categorical. These assumptions are violated when the number of variables evaluated is larger than the observation. These statistical methods also have problems working with missing data. The lack of a data element in the matrix forces the removal of the row and column that contains it. Also these methods are unable to handle information and experimental data that describe a phenomenon with multiples responses (Y) [1].

5.1.3 Multivariable data analysis.

Modern instruments employed in research have the capacity to analyze a sample acquiring information with thousands of variables in a short time, where the number of variables greatly exceeds the number of observations. This has become a problem for the classical method of statistics and it has originated the necessity of new techniques for data analysis.

The multivariable projection methods were developed to fill these needs. Among the most popular methods are the Principal Component Analysis (PCA) and the Projection to Latent Structure (PLS). These methods are appropriate to handle data

with many variables and few observations, deals with missing data, handles matrices of any size, the variables can be no independent, deals with the dimensionality of the problem, are robust to noise in X and Y, separates easily the regularity of noise, and deals with data not normally distributed [1].

5.1.3.1 Principal component analysis (PCA)

Principal component analysis is a projection model developed by Wold H. et al. in the 80's [1]. This model was developed to deal a data matrix X with O observations (rows) and m variables (columns). (See Figure 5.1)

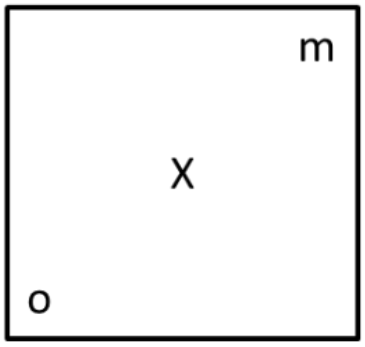

Figure 5.1 Data table for PCA model.

The analysis method of PCA is focused on the reproduction of the data in a dimensional space m employing the model $X=TP^T + \varepsilon$, with the finality of having the best description of the process based on obtaining the less residual error possible (ε). The representation of a data modeled in PCA can be observed in the Figure 5.2. In

the model the matrix T has columns with the score of matrix (t_1, t_2, t_3,…, t_a). The scores are new variables which condense old ones. In their derivation, the scores are fixed in descending importance (t1 explains more variation than t2, t2 explain more variation than t3, and so on). The mean of the scores is given by the loading matrix P (p_1, p_2, p_3…,p_a). Note that in P^T, T is for the transpose of the P matrix. The term A represents the number of principal component used to approximate the data table.

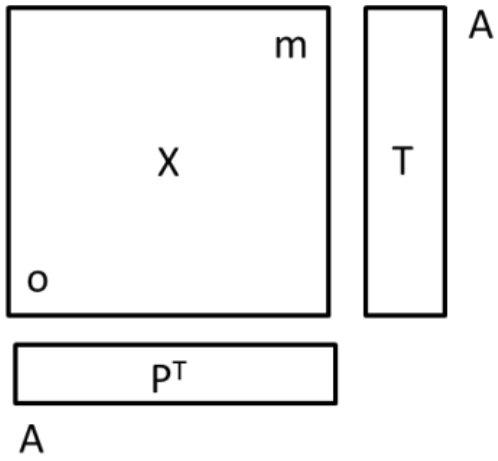

Figure 5.2 Data table modeled in PCA

PCA was developed to analyze data matrices with only one response, which makes this model limited to a few applications. Therefore, the statistical analysis developed in this research is the technique of projection to latent structures (PLS). This technique has shown great advantage to be implemented in different

scientific fields, because it has a reliable performance for the analysis of multivariable data with multiple responses.

5.1.3.2 Projection to latent structures (PLS)

The PLS method was developed around 1975 also by Herman Wold. This method was created for the handling of complex data sets with matrix techniques. Around 1980 the PLS model with two blocks (X and Y) was modified by Svante Wold et al. to be more suitable to data from science and technology. Since then the PLS has shown to be valuable to analyze complicated data sets where it is impossible or problematic to use traditional regressions [1-4].

PLS is a method that relates two matrices X and Y. The matrix X has a dimension (o x m) and the Y matrix has a dimension (o x n). The letters m, n and o correspond to the number of variables in X, number of responses in Y and number of observations in both blocks, respectively. (See Figure 5.3).

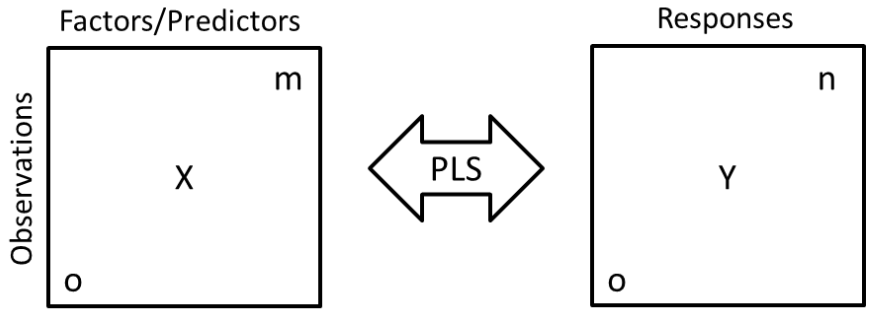

Figure 5.3 Data tables for PLS model.

The PLS method is appropriate to be implemented in the analyses of blocks of X and Y matrices with a lot variables, noisy collinear, and even incomplete information. The precision of the PLS method improves with increasing of the number of variables in the block X. The PLS is extremely advantageous to evaluate process or system where there is not fundamental theory well established, PLS-DA is the same PLS, but the responses are discrete [1].

In a process that requires a lot information to be described, the PLS method allows to easily find an interaction pattern among of the variables, and responses. In PLS the studied variables are related by aspect of a same fundamental characteristic.

The PLS multivariable method is represented in a general model with the following equations:

$$X = TP^T + E \quad \textbf{5.1}$$

$$Y = TQ^T + F \quad \textbf{5.2}$$

Where T is the score, P and Q are the loading of the matrix X and Y, respectively. The letter E and F are the error terms of the model respect to the variables and responses.

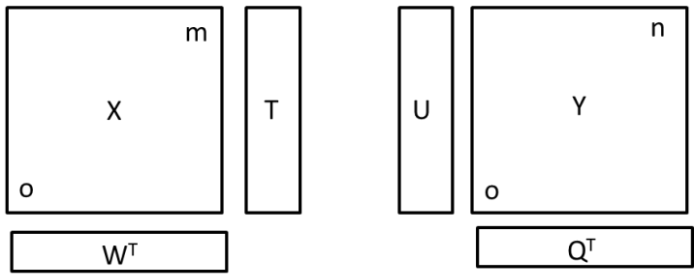

Figure 5.4 Data table modeled with in PLS.

The loadings and scores are obtained using the NIPAL algorithm and the numbers of principal components are selected by cross-validation [1].

5.1.4 Variable Important to the Projection

VIP (Variable important to the projection) is a term associated to the influence in Y of all the terms of X_k in the model. The larger of the VIP column in variables studied indicates the relevance of the variable in the process evaluated. Despite the fact that PLS is a proven tool to understand complex process and the analysis of problematic data, it is not a technique that has been reported in the analysis of the synthesis of nanostructures.

5.2 Methodology for Analysis of Results in Chapter 2

The input variables or factors in the X-block evaluated in the PLS-DA model were: type of platinum precursor, state of reducing agent, and synthesis

temperature. The Y-block output variables or responses in the obtained after the experimental procedures were: average size, standard deviation, and localization and morphology of the platinum nanostructure. The description and details of each variable are shown in Table 5.1. All of the mathematical calculations and results were computed employing the software Phi v 1.6.

The multivariable statistical analysis was developed using two principal components, the number of principal components was selected based on the best relationship between the X-block and Y-block obtained in the cross-validation. Using two principal components the correlations between the input variables and the responses were 98.0% and 60.0%, respectively.

Table 5.1 Details of the variables used in the multivariable analysis of the experimental section "Synthesis of supported Pt nanoparticles, multipod, nanoflowers, and nanowires in zeolite mordenite by varyng the metal precursor and the reduction methods".

Matrix	Variable name	Description
X	$Pt(NH_3)_4^{2+}$	positive platinum precursor
X	$PtCl_6^{2-}$	negative platinum precursor
X	StateRed. Agent.	Cohesiveness characteristic of the reducing agents: gas (low=1), liquid (medium=2), and solid (high=3).
X	Temp.	synthesis temperature
Y	Avg. Size NS	average size of the nanostructures
Y	StDev.	standard deviation of the average size of the nanostructure
Y	NC	nanostructures with morphology of nanoclusters
Y	NW	nanostructure with morphology of nanowires
Y	NF	nanostructure with morphology of nanoflowers
Y	Inside	position of the nanostructure (within the zeolite)
Y	Outside	position of the nanostructure (on the surface of the zeolite)

5.3 PLS Analysis of Results in Chapter 2

Figures 5.5 and 5.6 show the percentage of variability captured in the PLS-DA model for each variable in the X and Y matrix, respectively. Figure 5.5 shows that the first principal factor is associated to the type of the platinum precursor employed, while the second principal factor is related to temperature and the state of the reducing agent.

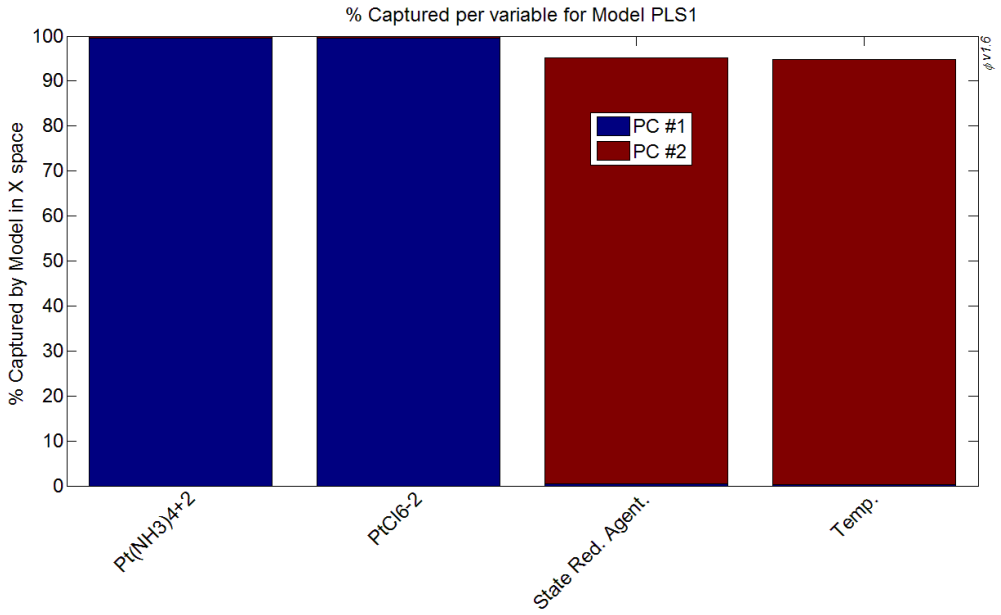

Figure 5.5 Percentage captured per input variable (X).

In Figure 5.6 it is clear that the first principal component influences all the Y responses and that the second principal component is more influential in the morphology and average size of the nanostructures.

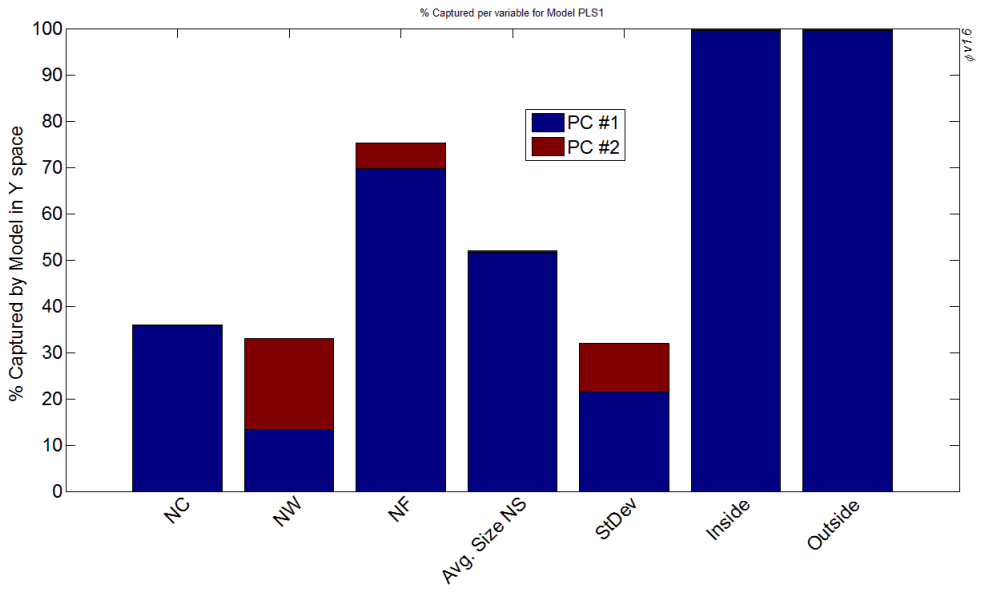

Figure 5.6 Percentage captured per response (Y).

Loadings of the PLS model are plotted in Figure 5.7. W1 and q1 loadings in the first principal component indicate that the formation of nanoclusters and nanowires inside of the zeolite is favored by the use of a positive platinum precursor, while the formation of nanostructures on the surface of the zeolite without control of the size and morphology is related to the use of a negative platinum precursor.

In Figure 5.7 the loadings w2 and q2 of the second principal component show that the temperature and the reducing agent are the factors that affect the formation of nanostructures with morphologies of nanoflowers, multipods and nanowires.

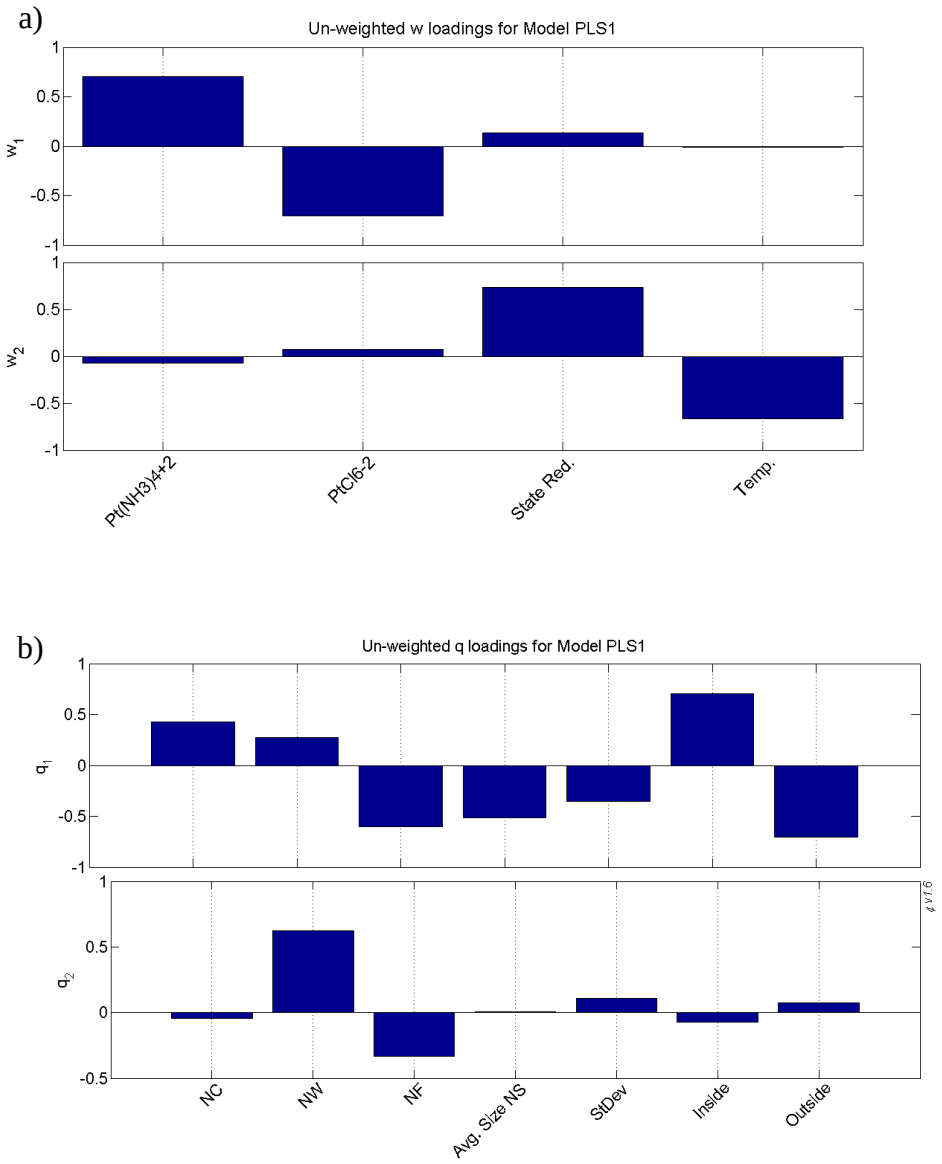

Figure 5.7 Loading plots for the variable: (a) Independent variables, "X" and (b) responses, "Y" in the PLS model.

The loading plots of the PLS model for the formation of nanostructures are very useful to identify the relationship between X and Y variables.

5.4 Methodology for Analysis of Solid State Reduction Method Results (Chapters 3 and 4)

General descriptions of the experimental conditions evaluated and the respective results obtained are reported in Table 5.2. These experimental results were used to develop the PLS-DA analysis. The independent variables (X) are: type of precursor, type of zeolite, and percentage of platinum. The responses of the experiment (Y) are: types of nanostructures, average size of the nanostructure, standard deviation, and location of growth. All of the mathematical calculations and results were computed employing the software Phi v 1.6.

The cross validation showed that with three principal factors the model achieves the best prediction. Employing the PLS-DA model with three principal components there is a correlation in the descriptive variables (X) of 96.4% and 91.1% for the responses(Y).

5.5 PLS Analysis for Solid State Reduction Method (Chapters 3 and 4)

Figures 5.8 and 5.9 show the percentage of variance expressed in the PLS model for each of the variables in the X (independent variables) and Y (response) matrices. The results shown confirm that the type of platinum precursor is essential to control the shape, size and growth of the platinum nanostructures [1, 3].

The second principal component is affected by the percentage of metal loaded in the zeolite. This component has a direct effect on the diameter of the platinum nanowires formed inside of the zeolites. (See Figure 5.8).

Table 5.2 Details of the variables used in the multivariable analysis of the experimental sections chapter 3 and 4.

Matrix	Variable name	Description
X	$Pt(NH_3)_4^{2+}$	positive platinum precursor
X	$PtCl_6^{2-}$	negative platinum precursor
X	Zeolite	ECR-5, MOR, VPI-5
X	Pt % wt.	Platinum loaded in the support (1, 3, & 5% Pt wt)
Y	Avg. Size NS[a]	average size of the nanostructures
Y	StDev.[b]	standard deviation of the average size of the nanostructure
Y	NC	nanostructures with morphology of nanoclusters
Y	NW	nanostructure with morphology of nanowires
Y	Inside[c]	position of the nanostructure (within the zeolite)
Y	Outside[c]	position of the nanostructure (on the surface of the zeolite)

a. Average size of the nanostructure correspond to the diameter of nanowires (NW) and nanoparticles (NC)

b. Standard deviation of the characteristic size of the nanostructures as defined in a.

c. Growth location of the nanostructures.

Figure 5.10 shows the VIP plot of the PLS model of this experimental section. In the plot the independent variables (X) are the platinum precursor, metal loading, and zeolite. The column heights represent the importance that the variables have in the construction of the PLS model that describes the shape, size and location of the nanostructures.

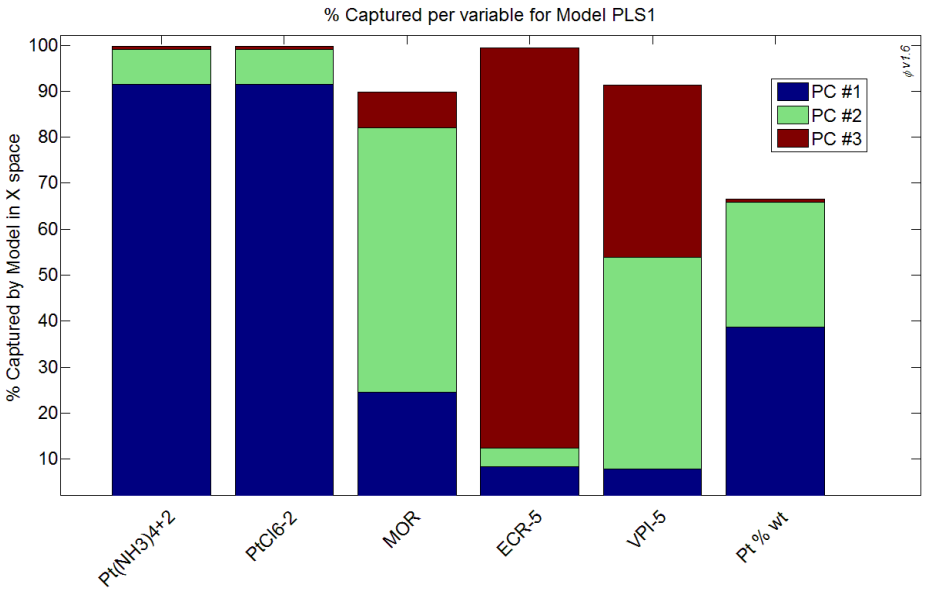

Figure 5.8 Percentage variance captured per independent variable (X).

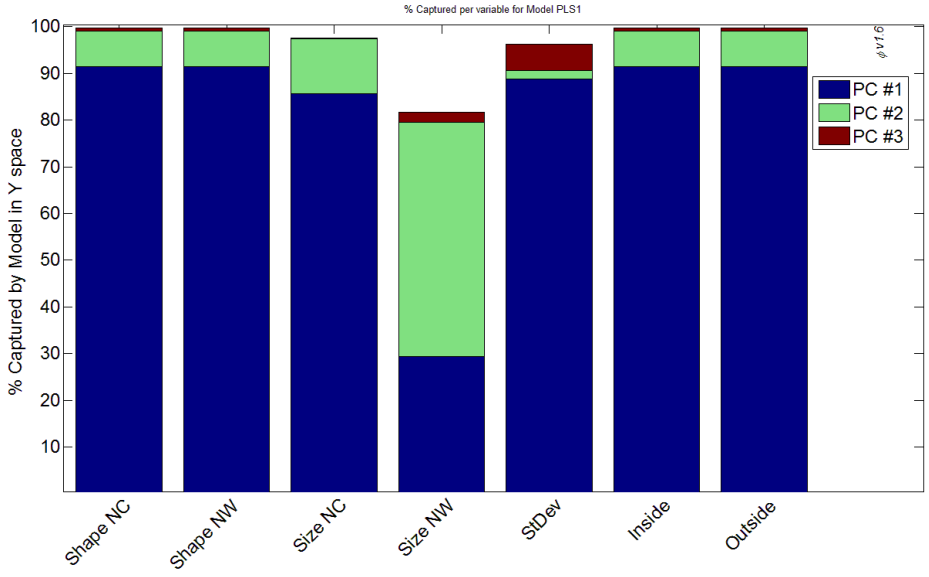

Figure 5.9 Percentage variance captured per the response (Y).

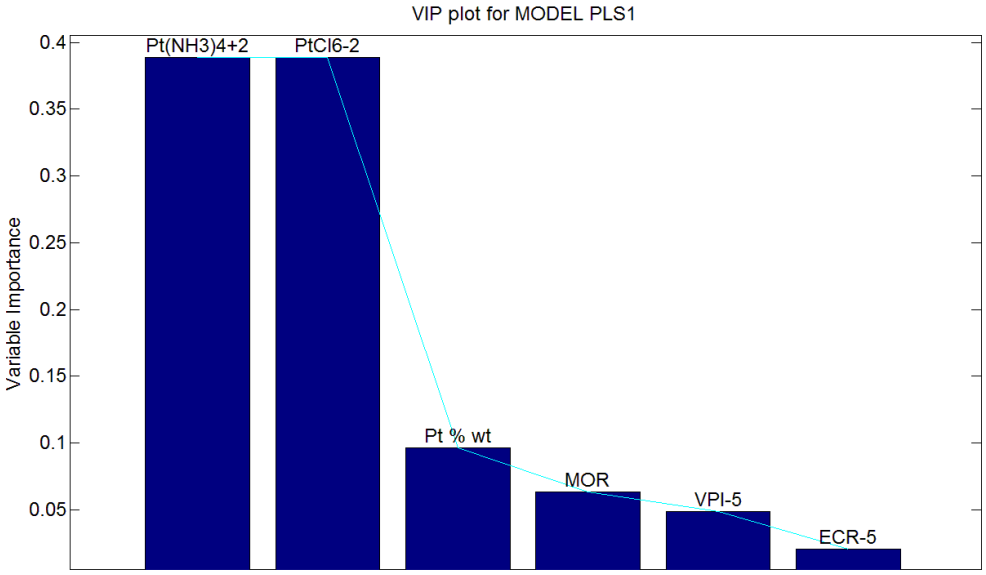

Figure 5.10 VIP plot for the solid state reduction method in PLS model.

The plot shows that the most important variable in this experiment was the identity of the platinum precursors; the concentration of the platinum was the second most important variable, and the variables least relevant to the experiments were the types of zeolite. This suggests that this method would be applicable to any zeolitic template and that the nanowire diameter could be controlled with Pt loading [3, 5, 6] .

5.6 Overall statistical analysis

This section presents an overall statistical analysis of the experiments in the previous sections, in order to identify the relevant variables in the formation of Pt nanostructures in microporous materials. The X variables (descriptor matrix) used in the multivariate statistical analysis were: type of precursor, zeolite, state of the reducing agent and temperature. The matrix (Y) variable responses were: type of nanostructures (nanoclusters, nanowires, and nanoflowers), average size of the nanostructure, standard deviation, and location of growth. These experiments were modeled using three principal components.

The experimental results are into the confidential limits of 95% and there are not the presence of outliers, this indicates that the experimental results are appropriate to be modeled by the PLS technique.

VIP analysis in Figure 5.11 shows that the type of precursor continues to be the factor of greatest influence in the synthesis process. The second most relevant variable is the reducing agent employed, followed by the reaction temperature, and finally is the zeolite. These global results agree with the individual observations and conclusions drawn throughout this dissertation and, while there were no surprises in the results qualitatively, these methods allows for the quantification of the relative importance of the synthesis variables have on the outcome of the experiments.

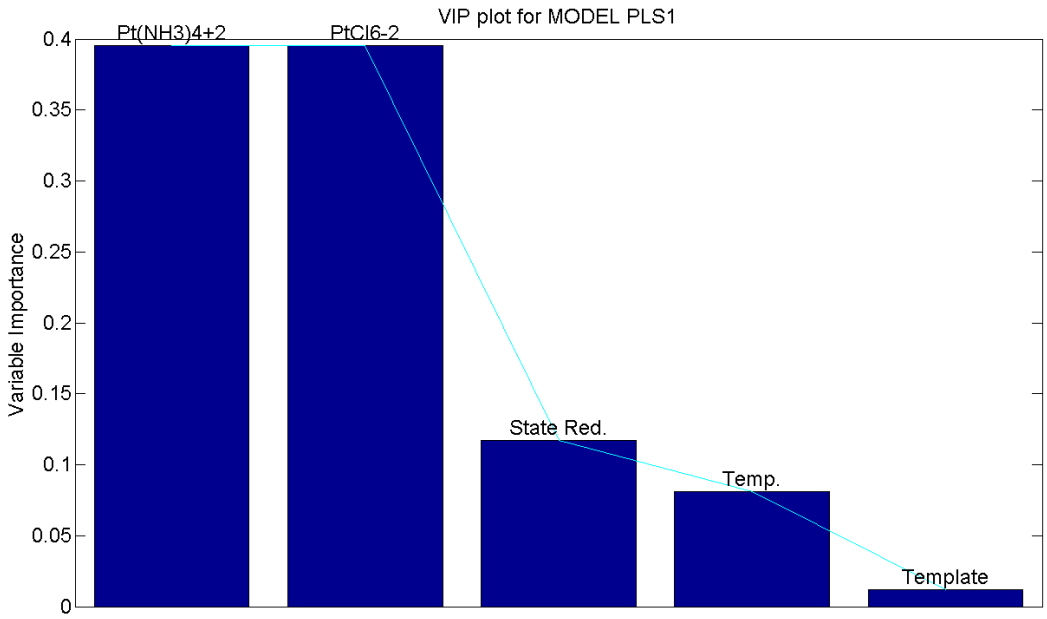

Figure 5.11 VIP plot in PLS model of overall formation of platinum nanostructures

5.7 Conclusions

In conclusion, in this chapter a suitable strategy was proposed to analyze synthesis processes of nanostructures using multivariate data analysis. The PLS-DA model provides a good understanding of the process by identifying the most important variables in the formation of nanostructures in zeolite and quantifying their relative importance.

References

[1] Eriksson L, Wold S (2006) Multi and megavariate data analysis. Principles and applications. Umetric AB, Sweden.

[2] Rao R, Lakshminarayanan S (2007) Variable interaction network based variable selection for multivariate calibration. Analytica Chimica Acta 599:24-35

[3] Garcia-Munoz S, Kourti T, MacGregor JF, Mateos AG, Murphy G (2003) Troubleshooting of an Industrial Batch Process Using Multivariate Methods. Industrial & Engineering Chemistry Research 42:3592-3601

[4] Chong I-G, Jun C-H (2005) Performance of some variable selection methods when multicollinearity is present. Chemometrics and Intelligent Laboratory Systems 78:103-112

[5] Berger-Karin CK, Evgenii V K (2010) Cellulose-templated materials for partial oxidation of methane: Effect of template and calcination parameters on catalytic performance. In: Studies in Surface Science and Catalysis Elsevier, pp. 635-638

[6] User Guide Simca P (2009), Umetric AB, Sweden

Chapter 6 CONCLUSIONS AND RECOMMENDATIONS

6.1 Conclusions

In this research new methods were established for the formation of platinum nanostructures with different morphologies: nanowires, multipods, nanoflowers and nanoclusters using zeolites. In the experiments, the use of reducing agents in gas, liquid, and solid state was evaluated for the platinum precursor/zeolite system for first time. The studies indicated that the dispersion of the formed platinum nanostructures decreases following the sequence of Gas>Liquid>Solid. This effect is attributed to the diffusive properties of the reducing agent.

Of special interest is the synthesis technique developed in this dissertation for the synthesis of nanowires in zeolites: the solid state reduction method. This is the first time that a solid state reduction method is used to form nanowires in a microporous material. The most important synthesis variables were identified for this synthesis method. It was found that platinum positively charged precursor such as the

tetra amine platinum (II) studied was necessary to incorporate the metal into the structure of zeolites in general.

For the formation of the nanowires, the amount of reducing agent was found to be a critical factor as with a low reducing agent/ Pt ratio no structures were formed. It was also found that with platinum concentration it was possible to control the diameter of the nanowires. In general these results demonstrated a novel synthetic way to form nanowires using zeolites that has the potential to be applicable to a wider range of metals, supports, and reducing agents.

In this dissertation a new strategy was developed to understand the growth process of nanoparticles in zeolites using multivariable analysis of data using PLS-DA. This is the first study in which a statistical technique "projection to latent structures" is used to understand the factors that are more influential to the morphologies and sizes in the synthesis of platinum nanostructures.

6.2 Recommendations

At the fundamental level it is still necessary to understand what is happening to the zeolite during the formation of the nanowires with solid state reduction. XRD results shown in Chapter 3 suggests a possible rupture of the zeolite but the use of complimentary techniques such as solid state NMR are necessary to understand this better.

It would be interesting in future to evaluate the formation of metal nanowires of gold, silver, and cooper using the solid state reduction method. Positively charged metallic precursors of these nobel metals exist commercially. As shown in this dissertation, these precursors would very likely incorporate into the zeolite to form templated nanostructures. In fact, our research group has already successfully employed the solid state reduction method to synthesize palladium nanowires in zeolite mordenite.

On the other hand, it would also be interesting to evaluate the use of the solid state reduction method in other supports. Preliminary experiments have shown that it is feasible, validating the idea for our proposed mechanism.

At the application level, characterization of the synthesized platinum nanostructures with cyclic voltammetry and in reaction systems at a laboratory scale would be necessary to understand their potential to be integrated in sensor devices and in the catalysis field, respectively.